POLITECNICO DI TORINO

Master of Science Program Energy and Nuclear Engineering

Master Thesis

An open source tool for energy planning of solar PV, wind and storage systems from long term time series for weather data

Supervisors: Candidate:

Prof. Filippo Spertino   Chandan Rajendra

Prof. Alessandro Ciocia

October 2022

Academic Year 2021/2022

Contents

Introduction

Energy has always been a fundamental aspect for the society. Nowadays many factors are contributing to the increasing and spreading of renewable energy sources, which are increasing energy demand, the decreasing availability of the fossil fuels, the increasing problems related to pollution and an unsustainable lifestyle. Photovoltaic technology represents an alternative with relatively highly efficient and good development opportunities.

In this thesis we concentrate mainly on building of an open-source python application which downloads the necessary data from the PVgis website for the calculation of productivity of solar PV plants and wind farms. Along with load profile as input, the self-sufficiency of the plant is also calculated by the software. The financial analysis is also done by the software using the inputs provided, and calculates the LCOE, NPV, PBT and IRR of the plant.

The most important part of this thesis is finding the optimal sizes/capacity of solar PV plants and wind farms for the selected co-ordinates to increase the self-sufficiency value by constraining the internal return rate. Optimization technique is carried out by the software by appropriate optimization methods which is further explained in this report.

.

1 General information about photovoltaic technology

1.1 The photovoltaic cell

Photovoltaic cell is an electronic device that directly converts the light energy into electricity by the photovoltaic effect, which is a physical and chemical phenomenon.

To understand this energy conversion process, we need to understand the photovoltaic effect. In this phenomenon, the photovoltaic cell absorbs light and this light energy is transferred to electrons and these electrons gets excited to higher energy level. This causes the production of electric potential by the separation of charges. For better understanding, Energy bands and electron-holes formation are explained below. [1] [2] [3] [4] [5] [6]

1.1.1 Energy bands

Electrons revolving in same orbit exhibit different energy levels. The grouping of this different energy levels is known as energy band. Band gap is defined as the minimum energy required for the electrons present in the outer most shells of the material to jump free from the parent atoms.

Different energy bands are explained below:

- Valence band is the outermost orbit of an atom;

When electrons absorb the light energy they get excited and jumps on to the conduction band. The difference of highest occupied energy level in valence band and lowest occupied energy level in conduction band is called as Band gap.;
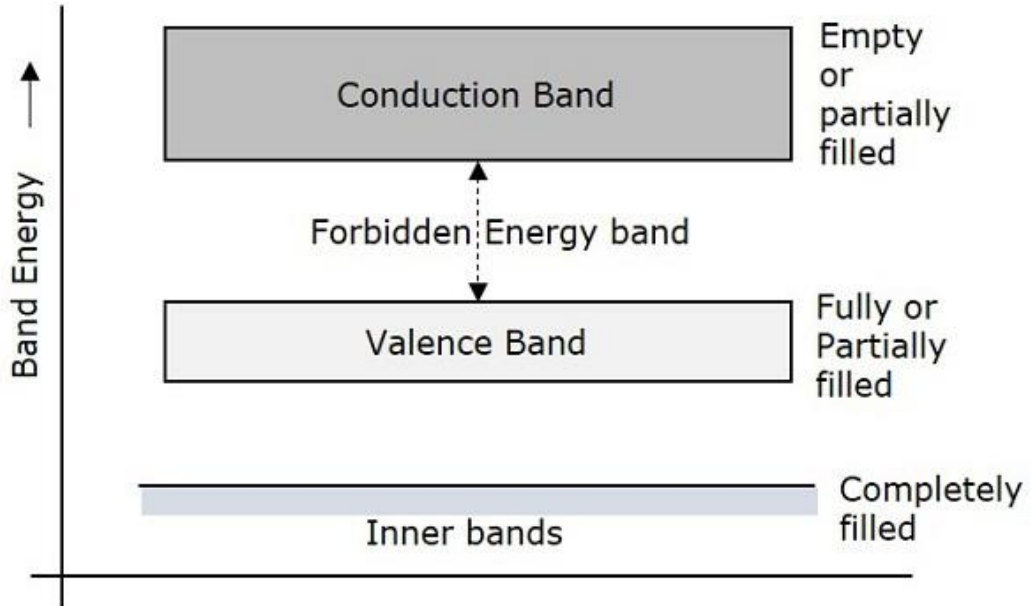
Figure 1-1: Energy bands in a generic material[9]

1.1.2 Classification of the materials based on Energy band

Based on Energy band materials are classified in three types:

- *Insulators:* These are the materials which do not allow current to pass through them.They have very high band gap or energy band, hence large amount of energy is needed to excite the electrons to conduction band.
- *Conductors:* These are the materials which easily conducts current. The valence band and the conduction band are overlapped, hence the electrons move easily to the conduction band;
- *Semiconductors*: These are the materials whose conductivity lies in between of Insulator and Conductors The energy gap is very small and very little energy is enough to excite the electrons form valence band to conduction band.[9]
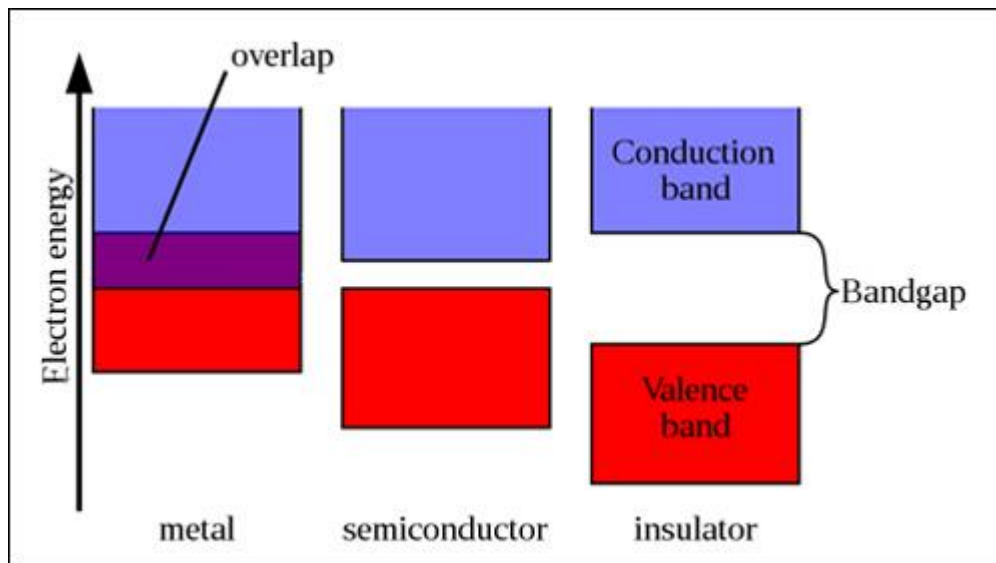
Figure 1-2: Comparison between Conductors, Insulators and Semi-conductors.

In Table 1 Energy band values of different semiconductors are listed.

Semiconductor	Energy gap [eV]
Crystalline Silicon (c-Si)	1,12
Amorphous Silicon (a-Si)	1,75
Germanium (Ge)	0,67
Gallium Arsenide (GaAs)	1,42
Indium Phosphide (InP)	1,34
Copper Indium Selenide (CuInSe)	1,05
Cadmium Telluride (CdTe)	1,45
Cadmium Sulphide (CdS)	2,4

Table 1: Energy band values of some semiconductors

It is provided in the following equation the equivalent Joule value of 1 eV:

$$1 eV = 1,60217646 \cdot 10^{-19} J \tag{1-1}$$

1.1.3 Photovoltaic effect

The photovoltaic effect is a phenomenon where current is produced in a semiconductor material when it is exposed to sunlight. In this phenomenon when the incident energy of the sunlight is larger than the energy band, an electron moves from the valence band to the conduction band by absorbing energy from incident sunlight. The energy of the incident photon in the sunlight is given by the below expression:

$$E_{ph} = h \cdot v = h \cdot \frac{c}{\lambda} \geq E_g \qquad (1\text{-}2)$$

Where,

- E_{ph} = Photon's energy [J];

- E_g = Energy gap [J];

- h = Planck constant ($6{,}625 \cdot 10^{-4} J \cdot s$);

- v = Frequency of radiation [Hz];

- c = Speed of light (300000 km/s);

- λ = Radiation wavelength [μm].

When the photon hits the semiconductor, the energy in the photons are transferred to the electrons in the valence band, and if the transferred energy is larger than the energy band the electrons gets excited and jumps to conduction band, during this process a hole is created in valence band, and this in turn creates an electron-hole couple.

After a short period of time the electrons returns to the valence band. The excess energy in the electrons is emitted in the form of thermal energy with no more energy conversion. [9]

1.2 Solar cell: structure and operation

Different types of solar cells are Single crystal wafers, Crystalline wafers and thin films. Crystalline silicon cells are most used in the photovoltaic market. Monocrystalline solar cells are more effective than the polycrystalline solar cells, but they are expensive. To reduce the cost, Polycrystalline silicon cells are more commonly used. These solar cells have very long lifetime equalling to 20 or more years and their production efficiency is reaching 18%. Amorphous silicon solar cells have less efficiency, but they are also less expensive. New type of thin film modules are produced and they are Cadmium telluride, which is also low cost and with acceptable efficiency. Whereas Gallium arsenide and Indium phosphide are used in space applications to power the satellites and in high intensity applications.

The solar cell forms the main component of the photovoltaic generator. It is nothing but a semiconductor diode whose shape depends on the type of the cell. The diode is placed between two electrodes. The top electrode is transparent to sunlight and allows the solar radiation to reach the cell. Second electrode is placed at the bottom. The thickness of the cell ranges from few micrometres to hundreds of micrometres.

The diode is created by the P-N junction between the electrodes. Silicon consists of 4 electrons in the valence band, "P-type" layer is formed by doping silicon with Boron. "N-type" layer is formed by doping silicon with phosphorus. Negative charges are distributed in "P-type" layer and positive charges are distributed in "N-type" player.
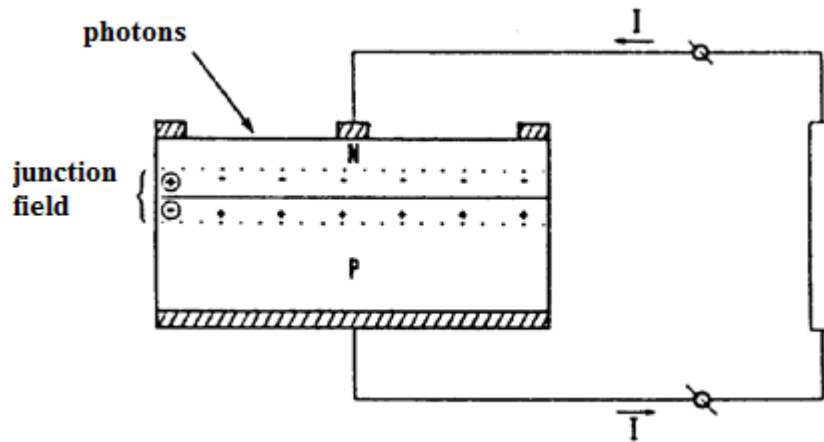
Figure 1-3: Structure of a p-Si solar cell

Bidirectional diffusion occurs when these 2 layers are made to come in contact. Electrons in the N-type layer diffuse to P-type, hole is created in the N-type region, similarly holes in the P-type region diffuse to N-type region thus creating electrons in the P-type region. This causes the formation of depletion region when two layers are made to come in contact with each other. The equilibrium is reached as an electric barrier is formed which stops further diffusion of holes to N-type and electrons to P-type region.

The equilibrium can be classified in two ways: *forward bias* and *reverse bias*. The forward bias is created by connecting positive side of the battery to the P-type and negative side to the N-type. This causes reduction of the depletion region, after sometime this depletion region gets vanished and current flows through the circuit significantly. Reverse bias is formed by connecting positive side of the battery to the N-type and negative side of the battery to the P-type. In this case the depletion layer gets bigger and bigger. And very small current flows through the circuit.[9]

1.2.1 Equivalent circuit of a solar cell

An ideal current source and an antiparallel connected diode represent a good approximation of the electrical operation of the solar cell.
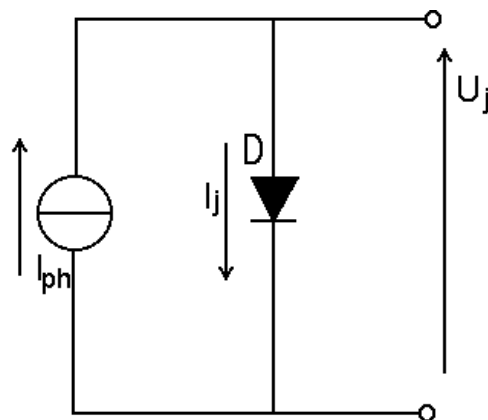
Figure 1-4: Ideal equivalent circuit of a solar cell

The the photovoltaic current that is generated through ideal current source is directly proportional to the surface area S and to the irradiance G, equation is given by:

$$I_{ph} = K \cdot S \cdot G \tag{1-3}$$

Where K = Coefficient that depends on the type of solar cell.

The behaviour of the rectifier of P-N junction is represented by the diode and the current flowing through the diode can be described with the help of the following equation (Shockley equation):

$$I_j = I_0 \cdot (e^{A \cdot Uj} - 1) \tag{1-4}$$

Where $-I_0$ = Reverse saturation current and U_j = Voltage that is measured at the terminals of the junction. The coefficient A is calculated through the below equation:

$$A = \frac{q}{m \cdot k \cdot T} \tag{1-5}$$

Where,

q = Electron charge [J],

T = Junction temperature [K],

m = Quality factor of the junction (it can vary between 1 and 2)

k = Boltzmann's constant $(1{,}38 \cdot 10^{-23} \, \text{J/K})$.

The equivalent circuit which describes the behaviour of the solar cell includes two resistances: Shunt resistance (R_{sh})which is connected in parallel and series resistance (R_s)which is connected in series to the circuit.

Figure 1-5 shows the real equivalent circuit of a solar cell.
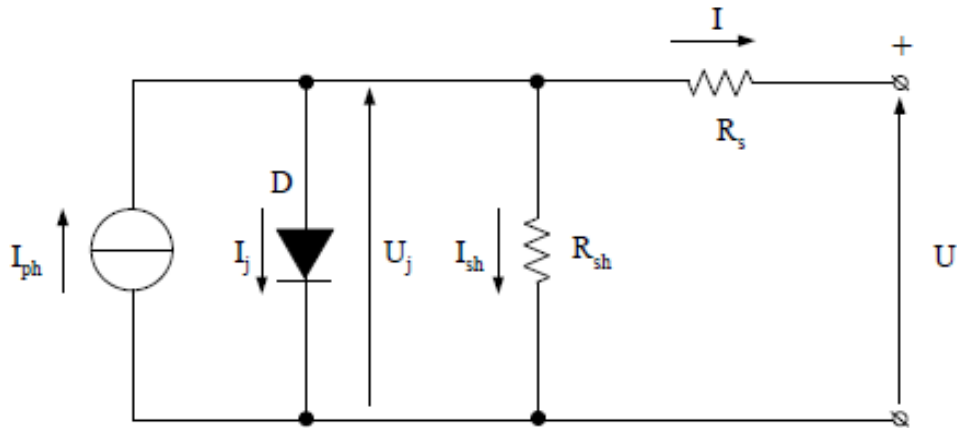
Figure 1-5: Real equivalent circuit of a solar cell

Kirchhoff's voltage and current laws are applied to the above circuit to obtain the voltage at the terminals of the load U and the current flowing through it. The following equations are written:

$$I = I_{ph} - I_j - U_j/R_{sh} \tag{1-6}$$

$$U = U_j - R_s \cdot I \tag{1-7}$$

U_j and I_j are calculated by the following equation:

$$U_j = \frac{1}{A} \cdot \ln\left(\frac{I_j + I_0}{I_0}\right) \tag{1-8}$$

$$I_j = I_{ph} - I - \frac{U_j}{R_{sh}} \tag{1-9}$$

In real time applications $R_s \ll R_{sh}$ and the term $\dfrac{U_j}{R_{sh}}$ are neglected, obtaining:

$$U_j = \frac{1}{A} \cdot \ln\left(\frac{I_{ph} - I + I_0}{I_0}\right) \tag{1-10}$$

Therefore, voltage U is calculated in the following way:

$$U = \frac{1}{A} \cdot \ln\left(\frac{I_{ph} - I + I_0}{I_0}\right) - R_s \cdot I \tag{1-11}$$

By imposing a specific value of current (I=0), The open-circuit voltage U_{oc} is obtained:

$$U_{oc} = \frac{1}{A} \cdot \ln\left(\frac{I_{ph} + I_0}{I_0}\right) \tag{1-12}$$

To obtain the current I we substitute the equations (1-7) and (1-4) in the equation (1-11):

$$I = I_{ph} - I_0 \cdot \left(e^{A \cdot (U + R_s \cdot I)} - 1\right) \tag{1-13}$$

By imposing specific voltage value (U=0), the short-circuit current I_{sc} is calculated:

$$I_{sc} = I_{ph} - I_0 \cdot \left(e^{A \cdot (R_s \cdot I)} - 1\right) \tag{1-14}$$

Since R_s, shunt resistance is the parameter that must be minimized in real applications it is neglected and the previous equation is written in the following form:

$$I_{sc} \approx I_{ph} = K \cdot S \cdot G \tag{1-15}$$

Therefore, the short-circuit I_{sc} is approximated as proportional to the surface area of the cell S and the irradiance G.

The following curve is obtained by neglecting the term $\dfrac{U_j}{R_{sh}}$ and it is the difference between the characteristic curve of the ideal current source and the real characteristic curve of the diode.
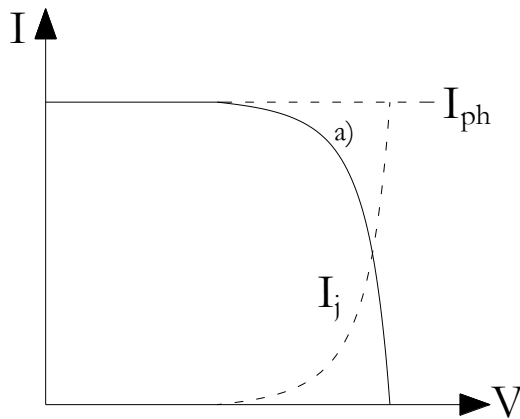
Figure 1-6: I(U) curve obtained by assuming R_{sh} infinite

If this term is not neglected, the slope of the curve in the horizontal part is larger and the intersection with the stress axis (I=0, corresponding to the idle state Uoc) shifts to lower stress values, as shown in Figure 1-7.
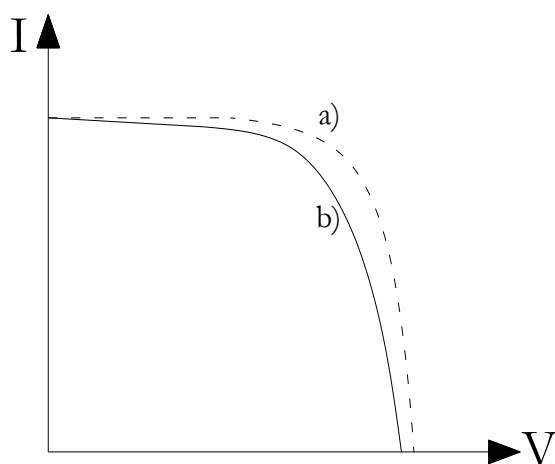
Figure 1-7: I(U) curve obtained with R_{sh} finite

Finally, the I(U) curve of the solar cell is obtained if we also consider the term: the slope of the vertical region is lower and the final curve is shown in Figure 1-8.
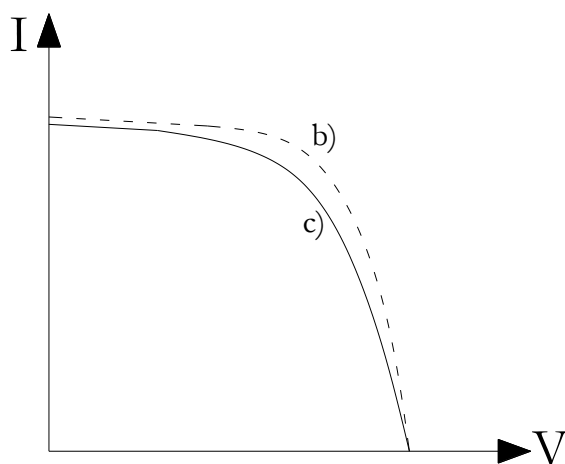
Figure 1-8: I(U) curve of a solar cell

The coordinates of the points forming this curve provide information about the electrical power that can be generated by the PV cell. Three points in particular are important: the no-load point (I=0 and U=Uoc), the short-circuit point (I=Isc and U=0), and the maximum power point (I= IM and U= UM), as shown in Figure 1-9.
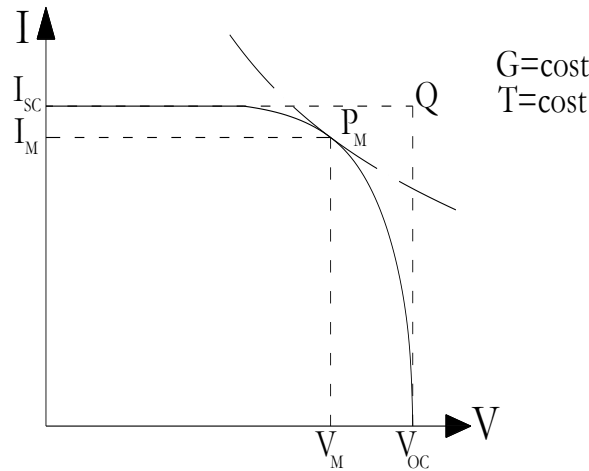
Figure 1-9: I(U) curve of the solar cell as a generator

The maximum electric power that can be generated by the cell is indicated by the maximum power point and it corresponds to the maximum area in Figure 1-9.

One of the very important parameters for photovoltaic/solar cells is the *Fill Factor* (K_f or FF), and it is defined as:

$$K_f = \frac{I_M \cdot U_M}{I_{sc} \cdot U_{oc}} \tag{1-16}$$

I_M is the maximum power current, U_M is the maximum power voltage, I_{sc} is the short-circuit current, and U_{oc} is the open-circuit voltage. This ratio accounts for the behaviour of the diode and the influence of the resistors R_s and R_{sh}. In general, a high value of FF indicates high solar cell performance. Common values of this ratio are between 0.5 and 0.8 and depend on the type of cell (higher values can be achieved with crystalline silicon technologies), up to 0.72-0.76, that correspond to ratios $\frac{I_M}{I_{sc}} \approx 0.9 - 0.95$ and $\frac{U_M}{U_{oc}} \approx 0.8$.

However, the complete form of the I(U) feature also extends to the quadrants II and IV. In these regions, the behaviour of the cell is different: it behaves like a load, with reverse voltage, $U < 0$ and $I > 0$, in the second quadrant and with reverse current, $U > 0$ and $I < 0$, in the fourth quadrant. The complete I(U) curve of a solar cell is shown as follows in Figure 1-10.
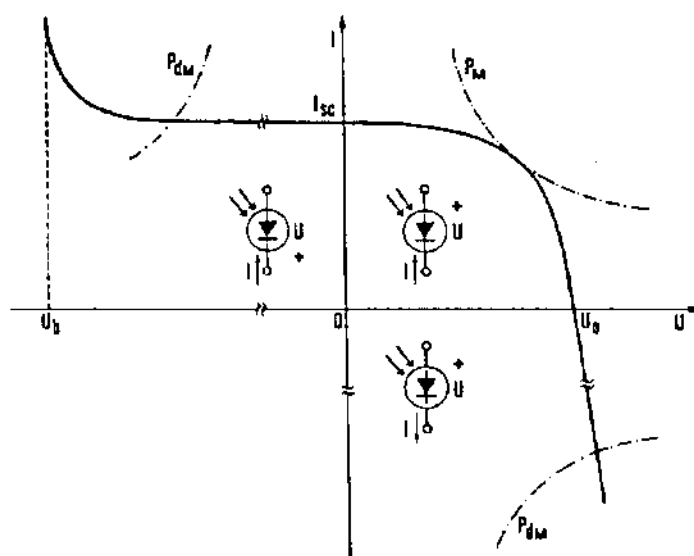
Figure 1-10: Complete I(U) characteristic curve of a solar cell

A fundamental aspect of solar cells, when they behave like a load, is failure due to high voltage. When the reverse bias voltage is too high and exceeds a threshold, called the *breakdown voltage* U_b, the cell is forced to dissipate too much thermal power and it fails, indeed a short circuit occurs. In general, a few volts are enough for silicon cells to cause the structure to fail.[1] [4] [5]

1.2.2 Dependence of irradiance and temperature

Two factors have a strong influence on the I(U) characteristic of the solar cell: the irradiance G and the temperature T . Figure 1-11 shows the dependence of the characteristic curve on the irradiance at constant temperature, and the maximum power points at the irradiance values considered are given.

Maximum power increases with increasing irradiance
Maximum power voltage changes little with irradiance

Current increases with
constant resistance

1000 W/m²

750 W/m²

500 W/m²

250 W/m²

Voc changes little
with irradiance

Current

Voltage

Constant
Temperature
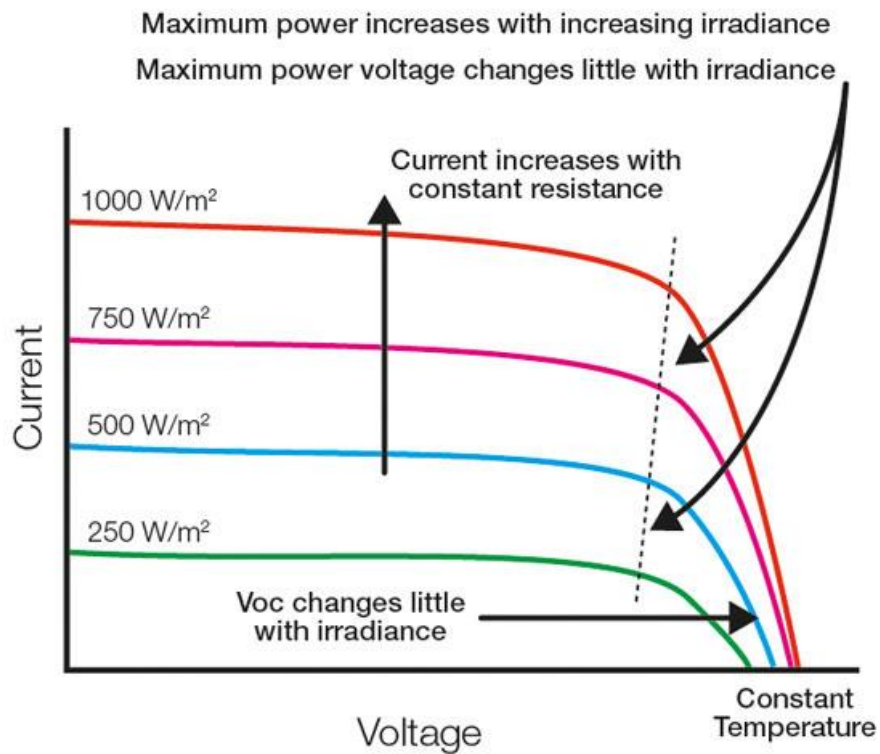
Figure 1-11: Dependence of I(U) curve on irradiance

Two effects are visible:

- The short-circuit current I_{sc} decreases proportionately as G decreases;
- The open-circuit voltage U_{oc} decreases logarithmically as G decreases, therefore it is almost constant and it decreases significantly only for very low values of G (less than 50 $\frac{W}{m^2}$).

Figure 1-12 shows the influence of cell temperature on its characteristic curve by keeping irradiance as constant.
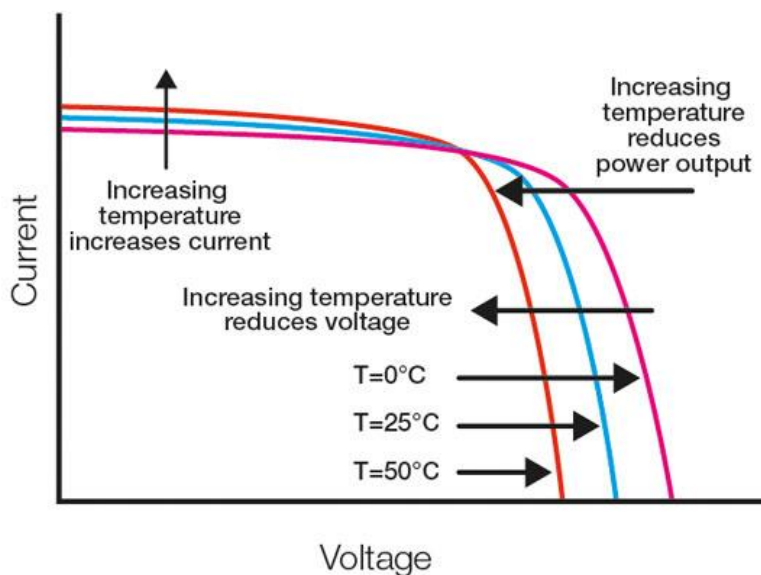
Figure 1-12: Dependence of I(U) curve on temperature.

It is possible to observe large fluctuations in the open-circuit voltage Uoc, while the short-circuit current Isc does not vary significantly. In detail:

- As the temperature increases, the band gap decreases and the photovoltaic current (and thus the short-circuit current) increases slightly;
- As I_j the diode current increases, U_{oc} the open-circuit voltage decreases (dU_{oc}/dT=-2,2 mV°C^{-1} for each solar cell).

As a result, the maximum power decreases with a almost constant thermal gradient defined by reference to the maximum power in the nominal state. This gradient is dP_M /dT 1/ P_{Mr} = -0.5%° C^{-1} for crystalline silicon technologies. Other values can be assumed for other types of solar cells, e.g., the amorphous silicon cells are characterized by smaller values of the thermal gradient of the maximum power.

In general, it is a reasonable approximation to consider the short-circuit current I_{sc} as depending only on irradiance and the open-circuit voltage as depending only on temperature.[9]

1.2.3 Losses in a solar cell

Losses in a Solar cell can be minimised but not completely avoided because the following factors affect the behaviour of the solar structure:

- *Reflection and coverage* of the surface of the cell. This type of loss occurs when some of the incident radiation is reflected or hits the frontal grating, and usually accounts for 10% of the total losses. To reduce this type of loss, anti-reflection coatings are applied to the surface of the cell and the surface area of the frontal grating is minimized;
- *Excess energy of incident photons* in the cell. This type of loss occurs when the photons incident on the cell surface have a higher amount of energy relative to the band gap of the semiconductor that makes up the cell. The additional amount of energy is lost in the form of heat. It usually accounts for 25% of the total losses;
- *Lack of energy* of incident photons over the cell. This type of loss occurs when the photons striking the cell surface do not have enough energy to create an electron-hole pair, and their energy is completely lost in the form of heat. This loss typically accounts for 20% of the total losses;
- *Recombination factor*. The recombination of electron-hole pairs can occur, and this phenomenon leads to the absorption of their energy in the form of thermal energy. The crystalline structure of the material (the presence of impurities and defects) strongly influences this loss, which can be up to 2% of the total losses;
- *Filling factor*. The diode and the resistors Rsh and Rs dissipate a considerable part of the electrical energy generated. In fact, it is not completely transferred to the external circuit, which leads to the typical distortion of the characteristic curve of solar cells with respect to the ideal rectangular shape. This type of loss can account for up to 20% of the total losses.[9]

1.2.4 Cell power and efficiency

Efficiency is defined as:

$$\eta = \frac{P_{MAX}}{P_i} \qquad (1\text{-}17)$$

Where P$_{MAX}$ [W] = Maximum electrical power the cell is able to produce, and P$_i$ is the incident irradiance, P$_i$= G·A on the surface area, A [m^2] of the PV cell. Conversion efficiency of PV cells that are available in the market can reach values up to 23%.

Figure 1-13 shows the profiles of the current density $J = \dfrac{I}{S}$ and the power density $p_u = \dfrac{P_u}{S}$ for a cell with surface area S, where P$_u$ is the useful power. These quantities are expressed as a function of the voltage U.
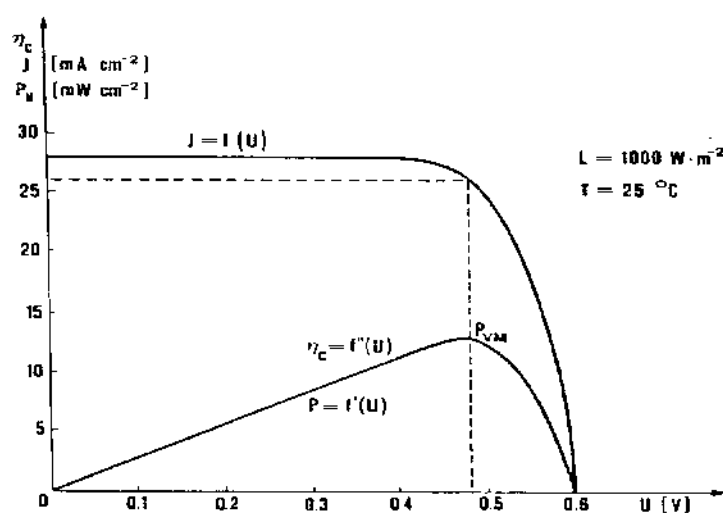
Figure 1-13: Dependence of current density J and power density p$_u$ on voltage U

Moreover, the conversion efficiency has the same characteristic as the power density p$_u$, since the input power P$_i$ is constant for a given geographical location and weather conditions.[4]

1.2.5 Series and parallel connections

Under optimal load and irradiation conditions, a single c-Si cell can produce a voltage value U = 0.5-0.6 V, which is almost independent of the amount of irradiated surface. The current, on the other hand, depends strongly on the surface area and typical values of short-circuit current density are $J_{sc} \approx 25 - 35 \dfrac{mA}{cm^2}$ ($I_{sc} \approx 4 - 5$ for cells with 12.5 cm side length and $I_{sc} \approx 6 - 8$ for cells with 15.6

cm side length). In real conditions, the voltage and current values required by the consumers are much higher, which is why series and parallel connections of several cells are necessary.

Multiple cells relate to two metallic contacts, one on the front and one on the back. The rear contacts completely cover the surface, as no active process takes place in this area, but on the front part of the cell the conversion process takes place, and it is necessary to have as large, irradiated area as possible, so a good compromise is chosen between complete permeability to radiation and maximum electrical conversion.[9]

1.2.5.1 Series connection

If N_s identical cells are connected in series (they form a "string") and one of them has an I(U) characteristic different from that of the other, the equivalent characteristic is equal to the sum of the voltage $(N_s -1)$ U of the N_s -1 cells under good conditions with the voltage U of the other cell for a given current. This is a typical example of a mutual deviation (mismatch) of the I(U) curve and may be caused by limited manufacturing tolerances or shading affecting specific areas of a system (or a single cell, as in the situation described).
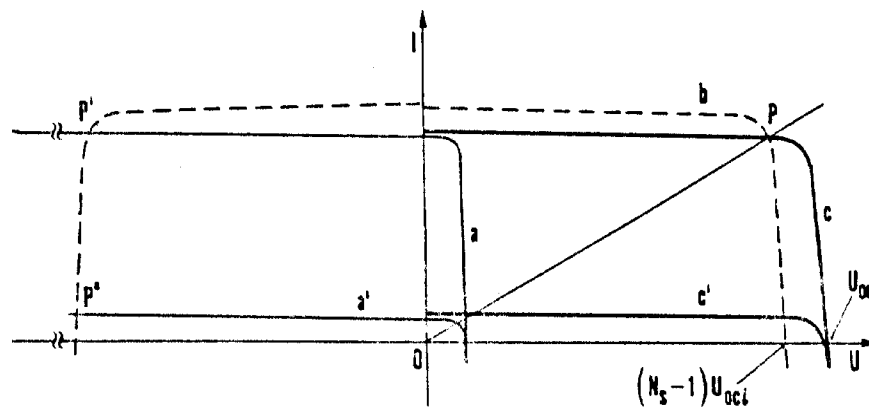
Figure 1-14: Characteristic curve of series-connected cells in mismatch configuration

In Figure 1-14 shows several curves representing the I(U) characteristics of the cells connected in series:

- Curve (a): Characteristic curve of cell with constructive defects.
- Curve (a'): Characteristic curve of shaded cell.

- Curve (c): I(U) curve obtained by sum of all the characteristics of the normal operating cells with curve (a).
- Curve (c'): I(U) curve obtained by sum of all the characteristics of the normal-operating cells with curve (a').
- Curve (b): characteristic curve of the N_s-1 good cells.

We note that the maximum power of the whole string in both situations is significantly lower than the corresponding curve (the point P is the point of maximum power) that can be obtained with N_s normally operating cells. In particular, the mismatch caused by shading has a negative effect on the production of the solar plant.[5]

Looking at the I(U) curve of the system, we can see that the open circuit voltage U_{oc} is the sum of the open circuit voltage U_{oc}, i of a single cell. The short-circuit current Isc, on the other hand, is almost equal to the minimum value of the short-circuit current Isc,i of the individual cells:

$$U_{oc} = \sum_i U_{oc,i} \tag{1-18}$$

$$I_{sc} \cong \left(I_{sc,i} \right)_{\min} \tag{1-19}$$

In the case of a fully shaded cell, the short-circuit current is zero (Isc=0) and it acts as a very resistive load. On the contrary, if the curve (a)/(a') does not deviate so much from the others, the reduction of the short-circuit current and therefore of the power that the system can generate is small.

When the value of the load resistance is lower than that corresponding to the operating conditions in P, cell (a) operates as a reverse voltage load. The most dangerous situation is the short-circuit at the terminals of the Ns cells connected in series, since the voltage (Ns-1) U is applied to the terminals of cell (a) and this voltage is the sum of the voltages of the fully irradiated cells. The points P' and P'' represents the operating conditions for the two configurations (constructive defects and shading, respectively) obtained with symmetry with respect to the current axis.

In this condition, the power that the defective cell must dissipate may be too high. In this condition, hot spots may occur and after a time depending on the extent of overload, irreversible rupture of the cell may occur. In particular, the limit value for a solar cell is the breakdown voltage U_b, and if the voltage of the Ns-1 cells

exceeds this value, immediate failure of the PV cell occurs. Typical values for the breakdown voltage are for a silicon cell, but since each cell can supply a voltage U 0.5 V, a series connection of 50-100 cells is required to damage the cell.

The best way to avoid the formation of hot spots is to connect a bypass diode in parallel to each cell (D_p). Figure 1 15 shows the configuration described, with the cells approximating ideal current sources
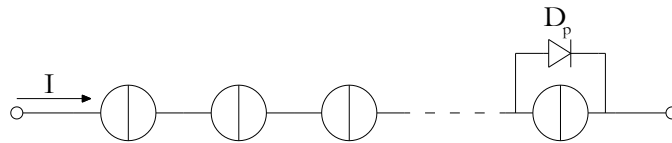
Figure 1-15: Parallel-connected protection diode

The role of the diode D_p is to limit the deviations from the ideal series connection, because it prevents the cell from acting as a load, and it avoids another very limiting aspect: the reduction of the short-circuit current I_{sc} of the system. The short-circuit current of the solar system I_{sc} is no longer equal to the minimum short-circuit current $I_{sc,i}$ between the cells, but is equal to the short-circuit current of the good cells connected in series. Consequently, the power reduction is limited to the contribution of the defective cell and is no longer so large that the system becomes inefficient (in the case of complete shading, the reference curve is curve (c')).

However, connecting a diode to each individual cell is not practical for terrestrial applications, and a good compromise is to connect a diode to rows of cells (usually groups of 18-24-36 cells are connected) that form a photovoltaic (PV) module.

In the case of cells connected in series with protection diodes connected in parallel, this can be observed:

- If a cell is interrupted, the string does not generate current.
- If a cell is shorted, the power generated by the string is reduced only by the contribution of the shorted cell.[4] [5]

1.2.5.2 Parallel connection

If Np identical cells are connected in parallel and one of them has an I(U) characteristic different from the others, the equivalent characteristic is equal to the sum of the currents of the Np-1 cells under good conditions with the current of the other cell for a given voltage.
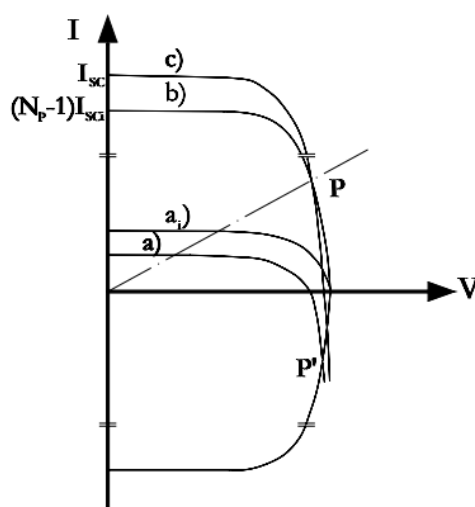
Figure 1-16: I(U) curve of parallel-connected cells

In Figure 1-16 shows several curves representing the I(U) characteristic of the cells connected in parallel:

- Curve (a): Defective cell characteristic curve.
- Curve (a_i): Single cell characteristic curve with good performance.
- Curve (c): I(U) curve which is obtained by summing all the characteristics of the good-operating cells with the curve (a);
- Curve (b): N_p-1 good cells characteristic curve.

The equivalent I(U) curve of the system has a short-circuit current value Isc, which is the sum of the short-circuit currents Isc,i of the individual cells. The open-circuit voltage Uoc, on the other hand, is almost equal to the minimum value of the open-circuit voltage Uoc,i of the individual cells:

$$I_{sc} = \sum_i I_{sc,i} \qquad (1\text{-}20)$$

$$U_{oc} \cong (U_{oc,i})_{\min} \tag{1-21}$$

When a cell is shaded, the parallel-connected cells operate similarly to the parallel-connected Np-1 cells in terms of load. Unlike the series connection, the open circuit is the worst condition: In this situation, the defective cell is forced to absorb all the current flowing from the normally operating Np-1 cells.

If the power consumption becomes too high, the excess temperature can cause damage to the cell. If the cell is damaged, it will stop working and the other Np-1 cells will start working in parallel again, but in general the parallel connection of single cells is not diffuse.

From the point of view of load, however, the influence of a parallel connection is less than that of a series connection.

The best theoretical solution would be to connect a diode Ds in series with each cell in parallel, since this configuration prevents the defective cell from operating as a load with reverse current. However, it can't be applied to the parallel connection of single cells, since the voltage drop across the terminals of a diode is approximately the same as that produced by the single cell. Therefore, it is more common to apply this protection circuit to strings of several dozen cells connected in series, as shown in the Figure 1-17.
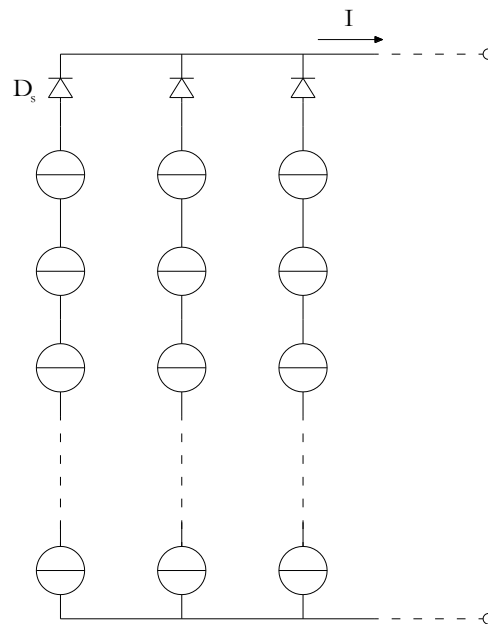
Figure 1-17: Series-connected protection diode

In both connections, however, the similarity of the cells is of fundamental importance. In fact, it is desirable that all cells have a similar I(U) curve (the coincidence of cells) to avoid the problems analysed. Therefore, the design of a module is very important and a careful selection of the cells (sorting) to be connected is required: in fact, it is preferable to use cells that have an I(U) curve as similar as possible.[4] [5]

Despite the sorting, some power losses cannot be avoided: The maximum power that the connected modules can produce is always lower than the sum of the maximum power of each module, and this deviation is about 2-3% of the nominal value.

Furthermore, the occurrence of external mismatches (e.g., shading) is not expected and cannot be avoided when sorting the cells.

1.2.6 The photovoltaic module

A PV module is a device consisting of several interconnected photovoltaic cells (e.g., 36 or 72) capable of converting incident solar radiation into electrical energy (photovoltaic effect). It is normally used as a power source in a photovoltaic system.

1.2.6.1 *Conversion efficiency of modules*

For a given irradiance G and temperature T, the power Ps incident on the surface A can be calculated as follows:

$$P_s = G \cdot A \tag{1-22}$$

If PM is the maximum power a module can produce, the global conversion efficiency of the module is:

$$\eta_M = \frac{P_M}{G \cdot A} \tag{1-23}$$

The total efficiency can be expressed as the product of the partial efficiencies:

$$\eta_M = \eta_P \cdot \eta_{EC} \cdot \eta_{IM} \tag{1-24}$$

Where:

- η_M = *global* efficiency of the module;
- η_P = *filling* efficiency;
- η_{EC} = *encapsulation* efficiency;
- η_{IM} is *not homogeneous irradiance* efficiency.

The filling ratio η_P takes into account that not the entire irradiated area of the module is suitable for energy conversion, but only the area occupied by the solar cells. It is therefore the ratio between the area occupied by the cells and the total area of the module; typical values for the filling ratio are around 85 %.

Encapsulation efficiency η_{EC} is calculated as the product of three terms:

$$\eta_{EC} = \eta_C \cdot \eta_T \cdot \eta_{MIS} \tag{1-25}$$

Where:

- η_C is the conversion efficiency of the cell without interlayer of the encapsulation resin and the cover glass.
- η_T is the optical efficiency of the glass and resin, which takes into account the absorption of solar radiation by the materials and is about 95%.
- η_{MIS} is an efficiency that, for a given value of irradiance, takes into account cell mismatch and losses due to the Joule effect in the resistances of the cell junctions. Typical values are around 95 %.

η_{IM} considers that the irradiance is not homogeneously distributed over the cells and typical values for efficiency are around 98%.

The conversion efficiency of a module is usually lower than the efficiency of the individual cells.[5]

1.3 Reference rated technical data and test conditions

1.3.1 STC Standard Test Conditions

According to technical standard IEC/EN60904, The characteristics of modules refer to STC (Standard Test Conditions).

- Irradiance G=1000 $\frac{W}{m^2}$;
- Air mass AM=1.5;
- Cell temperature T_c=25 °C.

1.3.2 NOCT, Nominal Operating Cell Temperature

The temperature at which the module is stable in open-circuit conditions and it can be evaluated with the following operating conditions:

- Irradiance G=800 $\frac{W}{m^2}$;
- Wind speed u_w=1 $\frac{m}{s}$
- Ambient temperature T_a=20 °C

NOCT (typical values are $42 \div 50°C$) helps us to calculate the temperature of the cell in different operating conditions. For a given irradiance G and ambient temperature T_a it is stated the difference T_c-T_a to depend linearly on the irradiance, for the following equation:[9]

$$T_c = T_a + \frac{NOCT - 20}{0.8} \cdot G \left[\frac{kW}{m^2} \right]$$
(1-26)

1.3.3 Power reduction

Power reduction can be expressed as a function of temperature with reference temperature equal to to 25°C,

$$\Delta P_m = \gamma_{Pm} \cdot (T_c - 25) \tag{1-27}$$

Where:

- ΔP_m is power variation [%] due to a cell temperature that is different from 25°C;
- T_c = Cell temperature [°C];
- γ_{Pm} = Power temperature coefficient, expressed as power variation in $\left[\dfrac{\%}{°C} \right]$.

1.3.4 Analytical approach for definition of cell parameters as function of temperature and irradiance

The main parameters of a cell are voltage, current and power, which strongly depends on the cell temperature and the irradiance. Many formulas describe the relationship of the cell temperature and the irradiance, and they are explained in the below paragraphs.[5]

1.3.4.1 Analytical expression of short-circuit current I_{sc}

The short circuit current as function of irradiance and self-temperature is given by the below relationship

$$I_{sc}(G,T) = I_{sc}(STC) \cdot \frac{G \left[\dfrac{W}{m^2} \right]}{1000} \cdot \left(1 + \alpha_{Isc} \cdot \Delta T \right)$$

With $\Delta T = T_c - 25°C$ \hfill (1-28)

Where:

- I_{sc} (STC) = The short-circuit current which is measured in STC conditions [A].

- G = The irradiance value $\left[\dfrac{W}{m^2}\right]$;

- α_{Isc} = short-circuit current temperature coefficient $\left[\dfrac{\%}{{}^\circ C}\right]$.

- T_c = Cell temperature [°C].

Temperature coefficient α_{Isc} can be also expressed in $\left[\dfrac{A}{{}^\circ C}\right]$.

$$\alpha_{Isc}\left[\frac{A}{{}^\circ C}\right] = \frac{I_{sc}(STC)[A]}{100} \cdot \alpha_{Isc}\left[\frac{\%}{{}^\circ C}\right]$$

(1-29)

1.3.4.2 Analytical expression of open-circuit voltage U_{oc}

Open circuit voltage U_{oc} is expressed as a function of temperature as expressed below:

$$U_{oc}(T_c) = U_{oc}(STC) \cdot (1 + \beta_{Uoc} \cdot \Delta T)$$

ΔT=T_c-25°C

(1-30)

Where:

- U_{oc} (STC) = open-circuit voltage at STC conditions [V] .

- β_{Uoc} = open-circuit voltage temperature coefficient $\left[\dfrac{\%}{{}^\circ C}\right]$.

- T_c = cell temperature [°C].

Temperature coefficient β_{Uoc} is expressed in $\left[\dfrac{V}{{}^\circ C}\right]$.

$$\beta_{Uoc}\left[\frac{V}{°C}\right] = \frac{U_{oc}(STC)[V]}{100} \cdot \beta_{Uoc}\left[\frac{\%}{°C}\right] \qquad (1\text{-}31)$$

1.3.4.3 Analytical expression of power P_m

Power P_m as a function of irradiance G and cell temperature T_c is expressed in the following way:

$$P_m(G,T_c) = P_m(STC) \cdot \frac{G\left[\frac{W}{m^2}\right]}{1000} \cdot (1 + \gamma_{Pm} \cdot \Delta T)$$

$$\Delta T = T_c - 25°C \qquad (1\text{-}32)$$

Where:

- P_m (STC) = The maximum electric power that is measured in STC conditions [W];

- γ_{Pm} = Power temperature coefficient $\left[\frac{\%}{°C}\right]$.

- T_c = cell temperature [°C].

Temperature coefficient γ_{Pm} is expressed in $\left[\frac{W}{°C}\right]$.

$$\gamma_{Pm}\left[\frac{W}{°C}\right] = \frac{P_m(STC)[W]}{100} \cdot \gamma_{Pm}\left[\frac{\%}{°C}\right] \qquad (1\text{-}33)$$

1.3.4.4 Analytical expression of the efficiency

The efficiency of the solar module is defined as the ratio of electric power which is produced by the cell and the total irradiance incident over this cell and it is given by the below expression[4]

$$\eta = \frac{P_m}{G \cdot A} = \frac{P_m(STC)}{A} \cdot (1 + \gamma_{Pm} \cdot \Delta T)$$

$\Delta T = T_c - 25°C$ (1-34)

Where:

- P_m (STC) = The maximum electric power that can be measured in STC conditions [W];

- γ_{Pm} = Power temperature coefficient $\left[\dfrac{\%}{°C}\right]$.

- T_c = Cell temperature [°C].

1.3.5 Data that are given by the manufacturer

For each module of solar cells the manufacturer provides the following data.

- Name and symbol of the manufacturer;

- Type and model number;

- Serial number;

- Polarity of terminals or conductors;

- Maximum operating voltage of the module;

- Module class of use;

- Class II symbol (for class A modules);

- Open-circuit voltage U_{oc} in STC conditions;

- Short-circuit current I_{sc} in STC conditions;

- Rated power P$_{rated}$ in STC conditions and indications on production tolerances;

- Maximum power voltage U$_{mpp}$ in STC conditions;

- Maximum power current I$_{mpp}$ in STC conditions;

- Maximum rated current of devices that protect the module against overcurrent (usually fuses);

- Cell temperature in nominal operating conditions (NOCT);

- Maximum tolerable reverse current;

- α$_{Isc}$, short-circuit current temperature coefficient expressed in $\left[\dfrac{\%}{°C}\right]$ or $\left[\dfrac{A}{°C}\right]$;

- β$_{Uoc}$, open-circuit voltage temperature coefficient expressed in $\left[\dfrac{\%}{°C}\right]$ or $\left[\dfrac{V}{°C}\right]$;

- γ$_{Pm}$, power temperature coefficient expressed in $\left[\dfrac{\%}{°C}\right]$ or $\left[\dfrac{W}{°C}\right]$

Normally, the maximum power Prated in is expressed $\left[W_p\right]$ only to briefly indicate that it is the maximum power. However, the module can produce more than Prated if the irradiance on the surface is higher than 1000 $\left[\dfrac{W}{m^2}\right]$, especially if the cell temperature is below 25 °C.[9]

1.3.6 Type tests and certifications

Some type tests (involving a batch of production) are coded in order to evaluate correctly modules performance during their lifetime (at least 25 years) that is simulated with artificial aging:

- CEI EN 61215 (crystalline silicon) or CEI EN 61646 (thin films) and they are characterized by the following procedures:

  o Visual inspection;

  o Performance in STC conditions;

  o Insulation test;

  o Measurement of α_{Isc}, β_{Uoc} and γ_{Pm} coefficients;

  o NOCT measurement;

  o Performance at NOCT temperature;

  o Performance with low irradiance;

  o External exposure test;

  o Localized overheat tightness test;

  o UV resistance test;

  o Thermal cycles test;

  o Humidity and freezing test;

  o Damp heat test;

  o Terminals robustness test;

  o Buckling test;

  o Mechanical loading test;

  o Hail test.

For the thin films modules, the following tests are provided according to CEI EN 61646:

- Prolonged exposure to light.

- Annealing.

- Leakage current test in damp environment.

In general, the active parts of PV modules used in grid-parallel supply systems must be class II -insulated. Double insulation is a combined protection against direct and indirect contacts and is symbolised as follows:
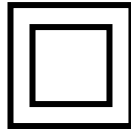
Figure 1-18: Symbol of class II insulation

Manufacturing warranty is the most important quality required and it is of 2 types.

- Product warranty against manufacturing and material defects, which must last at least 2 years.

- Power guarantee against power degradation. The measured power in STC shall not be less than 90% of the minimum power for at least 10 years and not less than 80% of the minimum power for at least 20 years.[9]

1.3.7 Protection devices

The I(U) curve of a PV generator has the same shape as the single cell curve, only the scales are different. As already explained for single cells, series and parallel connections can reduce the generated power and create "hot spots" caused by asymmetries in the I(U) characteristic (mismatch).

This phenomenon is caused due to:

- Intrinsic diversity of I(U) characteristic curves.

- Shading effect.

Hence for this reason, it is important to use necessary protections.

1.3.7.1 Protection diodes

In a series of modules connected in series, a protection or bypass diode Dp is connected antiparallel to each module (or to a group of cells - 18 or 24 - within the module). The diode has two positive effects:

- Protects the shaded cell from reverse voltage;

- It stops the string from producing and it is limited by the contribution of single module.

In Figure 1-19 we can observe how protection diodes are connected to PV modules.
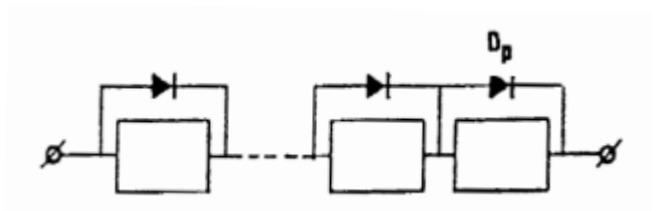
Figure 1-19: Protection diodes

To protect modules connected in parallel from asymmetries, a protection diode D_s is connected in series with the module, or the series of modules connected in series. Current generated by the module (or modules) flows in the diode and, because of its threshold (0.6-0.8 V), it generates a voltage drop that must be negligible relative to the voltage generated by the module (or modules) to limit power losses in the system. If one or more cells in a string are defective, there is an unbalance in the open-circuit voltage between the strings connected in parallel, which is why the diode D_s acts like a barrier. The string is not damaged, but it does not produce current. However, this situation is rare if the operating voltage is sufficiently lower than the open circuit voltage: In systems with MPPT devices, the operating voltage is about 80% of the open circuit voltage, and it is possible not to

use protection diodes connected in series with the modules. In addition, in the absence of solar radiation, the D_s diode protects the modules from the absorption of reverse current due to external electromotive forces generated by accumulators, motors, etc.

In Figure 1-20 one can observe how protection diodes are connected in series with modules connected in parallel:
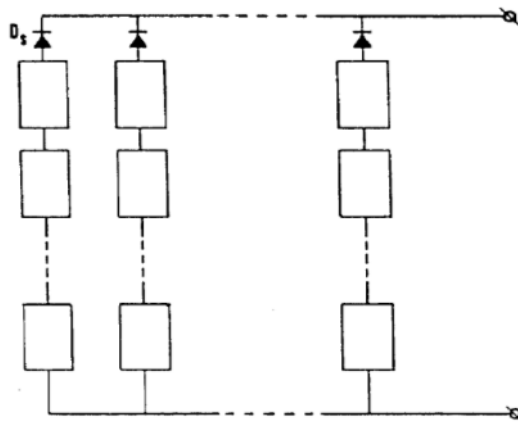
Figure 1-20: Protection diodes in parallel with series-connected modules

1.3.7.2 Possible configurations

When designing a photovoltaic generator, it is very important to choose the optimal connections between the modules, i.e. the configuration of the PV system, because this choice greatly affects the performance and reliability of the generator, with disturbing factors such as.

- Non-uniformity of cell parameters.

- Random shading.

- Deterioration of materials.

- Breakdown.

- Lightning strikes.

- Others.

Several configurations of PV systems are possible, but there is no clear and simple method to choose the best configuration (with the best performance). In this case, the boundary conditions (constant voltage at the load, minimum power losses, etc.) are fundamental to design an efficient system.

The most common configuration is the parallel or row configuration. In this case, with a shaded cell, the voltage delivered to the load is not affected, but the power contribution of the string is lost. Figure 1-21 shows the configuration.
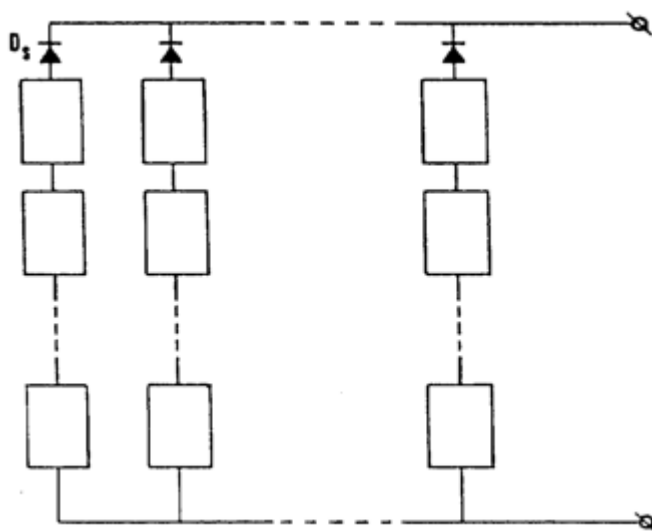
Figure 1-21: Parallel of series configuration

In the parallel connection, only one protection diode Dp is connected in parallel to each string instead, but it must withstand a higher current value. Figure 1-22 shows such a configuration.[9]
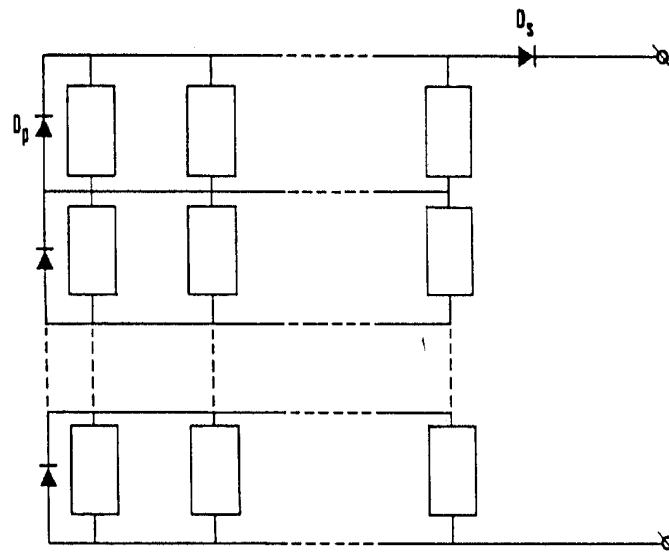
Figure 1-22: Series of parallel configuration

1.3.7.3 Connection with loads

The I(U) characteristic of modules is similar to that of single cells. However, it refers to a rescaling process that takes place on either the current or voltage axis.

A characteristic curve of 36 series connected cells module along with irradiance $G=1000$ W/m^2 and temperature T=25 °C is shown in Figure 1-23.
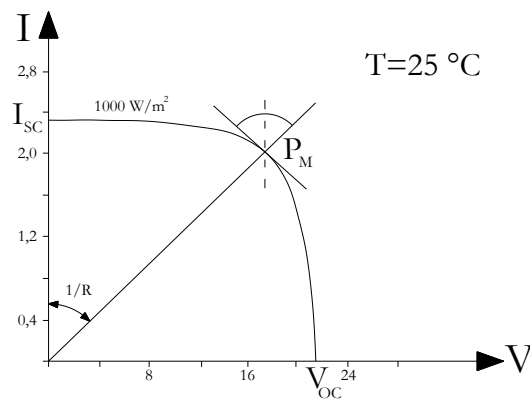
Figure 1-23: Typical I(U) curve of a photovoltaic module

The operating point is determined by the intersection between the I(U) characteristic curve and the curve of the connected load. Two relevant conditions are the short-circuit condition (I=Isc and U=0) and the no-load condition (I=0 and U=Uoc). In addition, it is possible to approximate the behaviour of the photovoltaic generator depending on the working range: In the range Isc-PM (PM is the point of maximum power), the PV generator can be considered with good approximation as an ideal current source, while in the range PM-Uoc, an ideal voltage source can approximate the behaviour of the PV generator.

The optimal operation point for a PV generator is its maximum power point PM. This is because connecting an adequate load will allow it to fully exploit the power generation performance.

In Figure 1-23 the load is a purely reactive load, and an optimal resistance value is required in order to achieve the maximum power. The I(U) curve is shown to be equal to the 0-PM slope.

$$\frac{dI}{dU} = \frac{1}{R} \qquad\qquad (1\text{-}35)$$

The temperature and irradiance of single cells are also taken into account to determine the optimal operation point for a PV system. In Figure 1-24, the effects of both temperature and irradiance are shown. The maximum power points locus is shown to be almost vertical. With a decreasing irradiance, both the short-circuit current and the open-circuit voltage are almost constant.[9]
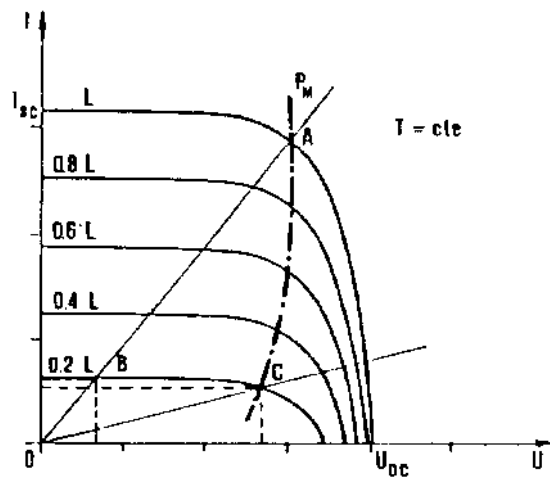
Figure 1-24: Influence of irradiance on maximum power point

By changing the temperature, the max power point locus becomes an area which is favourable for working.[9]
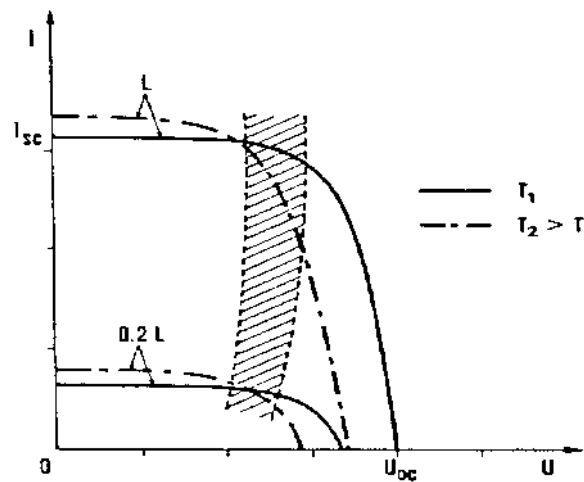
Figure 1-25: Influence of temperature on maximum power point

1.4 Electroluminescence

One of the most widely used methods for analysing the degradation of photovoltaic systems is the electroluminescence test. This method involves the

emission of photons from the atoms in the modules. Unlike other methods, this method does not cause any mechanical or electrical damage. [7]

1.4.1 Operating principle

It is based on the principle of electroluminescence. Some materials, mainly semiconductors, can emit photons when an electric current is applied. In normal operation, the PV module converts solar radiation into electricity, but in electroluminescence, an external voltage is applied to the module, causing current to flow through the module and emitting infrared radiation. You can use the images you take to distinguish between normally functioning cells and defective cells. In particular, the high-intensity areas show no damage, but the low-intensity cells appear dark (usually gray or black) and are damaged or electrically insulated. In addition, the main advantages of this method are:[4]

- Simplicity .
- Ability to realize high resolution mappings with short acquisition times.
- Possibility of applications in industrial scale.
- Possibility of integration with other analysis methods.
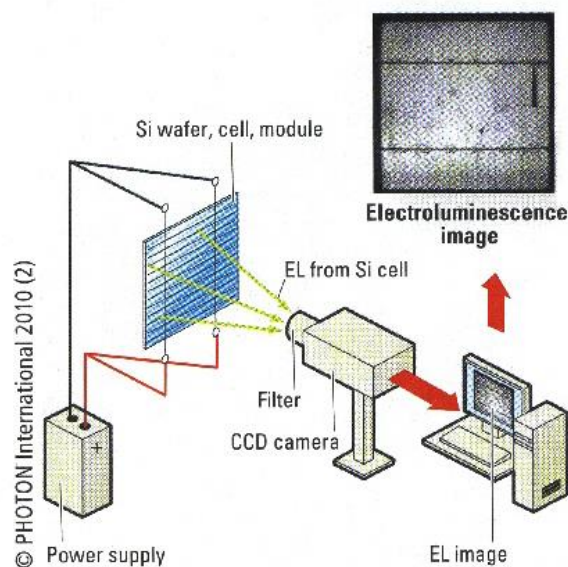
Figure 1-26: EL analysis of a PV module

1.5 Components of a photovoltaic system and mismatch

Solar modules can generate power in the order of hundreds of watts. Therefore, multiple modules must be interconnected to increase the output power. Connections between modules can be in series or in parallel. Several interconnected modules form a string with the same total voltage.

$$U_{string,max} = \sum U_{OC,i}$$

An array is a parallel connection between several strings.

Each solar module has its own characteristics. However, there are several factors that cause differences between different modulus curves. Among the most important, it highlights constructive differences between modules or different operating conditions caused by local phenomena such as shading. Differences between different characteristic curves are called mismatches and cause loss of performance and efficiency. Mismatches can occur in both series and parallel circuits, so protection systems are required to avoid these conditions. In a series circuit, if the characteristics of one cell differ from the other cells, the voltage is the sum of the voltages of the individual cells, but the currents flowing must be the same that of a failed module.

$$U_{tot,series} = \sum_{i}^{n-cells} U_i$$

(1. 1)

$$I_{tot,series} = I_{min}$$

(1. 2)

In parallel connections, there are two cases, i.e., the total current is given by the sum of the currents, but the voltage is equal to the voltage of the faulty module.

$$I_{tot,series} = \sum_{i}^{n-cells} I_i$$

<div align="right">(1. 3)</div>

$$U_{tot,series} = U_{min}$$

<div align="right">(1. 4)</div>

The most important protection system is a diode, an element that allows current to flow in only one direction. In series connections, the anti-parallel bypass diode (Dp) eliminates the worst cell effects without affecting the overall performance of the connection. On the other hand, in parallel connection, the blocking diode D connected in series with each string has double operation but is connected in series with a very large group due to the voltage drop due to the threshold voltage. Of cells. Therefore, the threshold voltage is negligible.[9]

1.6 Estimation of production

Photovoltaic systems can generate electricity with direct current. Knowing the climate data of the site to be analysed and the characteristics of the modules installed will be very helpful in estimating the productivity of the plant.

$$E_{AC} = H_g \cdot S_{PV} \cdot \eta_{STC} \cdot PR$$

$$E_{AC} = P_N \cdot h_{eq} \cdot PR$$

In the formulation of first equation, Hg is the global irradiance, S_{PV} is the area of the photovoltaic cell, $\cdot \eta_{STC}$ is the efficiency calculated under standard conditions, and PR (Performance Ratio) is a dimensionless parameter and consider various sources of loss.

$$PR = \eta_{mis} \cdot \eta_{d,r} \cdot \eta_{spect} \cdot \eta_{wir} \cdot \eta_{temp} \cdot \eta_{shad} \cdot \eta_{PCU}$$

Intrisic mismatich — AM ≠1,5 — T ≠25 °C — DC to AC convertion

dirt and reflection — wiring and blocking diode — shading effect

This formula represents the main cause for all the losses that determine the value of the Performance Ratio. This parameter varies between 0.55 and 0.85.

In first equation, productivity is calculated from the rated power of the module under normal conditions and the equivalent time value. This last parameter is defined as the ratio of solar radiation to irradiance and indicates the number of hours the system is operating at rated power during a given time interval.[9]

1.7 State of art and future

Monocrystalline silicon is the most common element among semiconductors used in solar cells. This element is very difficult to find in nature in its pure form. In fact, it is extracted from silica by various chemical processes. Polycrystalline silicon, on the other hand, is obtained from electronic waste. Amorphous, on the other hand, does not have a crystalline structure like the first two. In the process, some silicon atoms bond to hydrogen atoms. Modules made of this material cost less than crystalline modules.

Other PV cells are instead made of indium-copper-selenide (CIS) and indium-copper-gallium-selenide (CGIS), which are made by stacking different materials. It makes better use of the solar spectrum by using materials that can capture different wavelengths of electromagnetic radiation, reducing energy loss from wasted photons.

Some of the most economical modules on the market are those made from Teredo-Cadmium (CdTE). This is because the materials used are derived from waste from other industrial processes. Among the modules with the highest efficiencies above 30% are those made from gallium arsenide (GaAs). However, the cost of these modules is not suitable for commercial use.

This technological innovation includes organic cells made from polymeric materials, which allows for lower cost realization of the structure. Another advantage is the ability to represent different colours (not just black) for easy use in architectural applications. The drawback of this technology is that it still has poor performance compared to commercial competitors. On the other hand, other innovations continue to be related to silicon, this time used for structures and thin films, which are thinner and can also generate higher power compared to traditional cells.[9]

1.8 Connection with the load

Unlike conventional generators, it is not possible to regulate the input power in photovoltaic generators, and power control is much more complicated. Therefore, in such systems the load adapts to the generator. Based on irradiation and temperature conditions, the maximum output power under these conditions can be determined in the PV system characteristic curve.

1.9 Inverter

Photovoltaic systems can generate electricity from direct current, but most end users require alternating current. In addition, the current must be alternating current and comply with certain technical standards to connect to the distribution network. To do this, you need to use an inverter, which is a DC / AC converter. This system can generate AC power at 50 Hz (for systems installed in Europe). The switching process is done via antiparallel switches and diodes. The switch can be of Mosfet or IGBT type and its movement is active at a specific frequency, the so-called switching frequency. It is produced by comparing sine waves of the same frequency, thanks to PWM technology (pulse width modulation). The waves generated by the bipolar triangle wave create a square wave that controls the switch.

Below figure shows a diagram of an inverter, and the *Figure 1.9* shows the PWM comparison technique, with which the switching signal is generated.[7] [8]
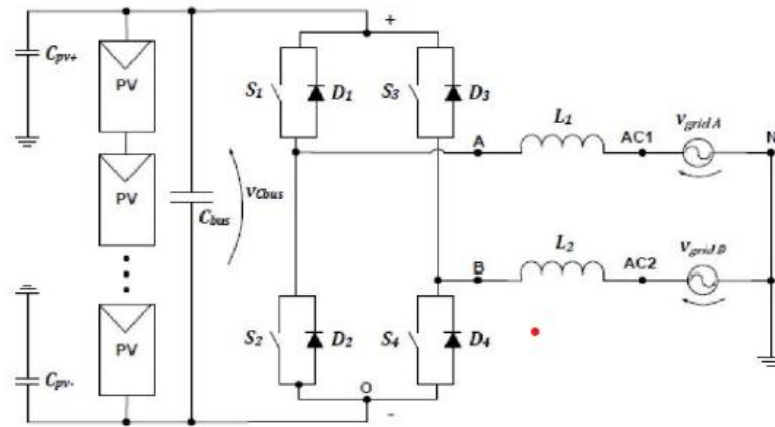
Figure 1-27 Diagram of Full bridge Invertor
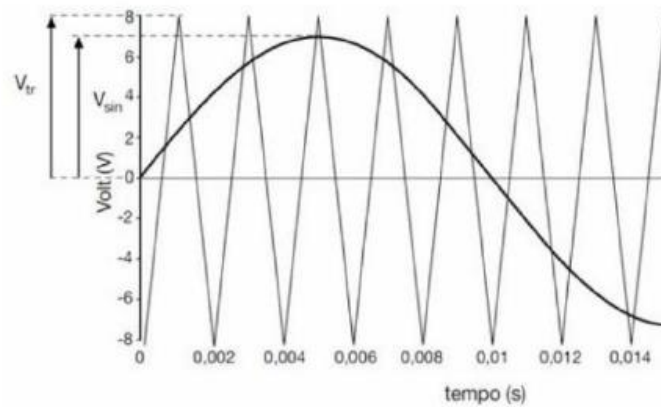
Figure 1-28 Pulse width modulation

2 General aspect of Wind Turbine

A wind farm (WT) is a plant that can convert the kinetic energy of the wind into electrical energy. Wind energy is considered a renewable energy source as it is inexhaustible and produces no air pollutants during operation. These systems make it possible to generate energy in remote areas without using fossil fuels. The main drawbacks of this technique are related to wind variability and difficulty in predicting sources. Other drawbacks are the visual impact and noise pollution that limit the installation of these systems.

2.1 Characterization of the wind source

Solar radiation hitting the Earth is not perfectly balanced, resulting in warmer regions near the equator and cooler regions at the poles. The earth also moves around the sun and rotates around a fixed axis. These mechanisms cause large amounts of air movement to move from one part of the Earth to another. In addition to these phenomena, other effects must also be considered, such as the pressure difference between the regions under consideration and the Coriolis effect. The movement of these air masses can be used to generate electricity.

Local effects alter wind propagation. These include surface roughness, ground elevation, and the presence of obstacles such as buildings and trees.

Wind speed and direction are measured with an anemometer. These systems use different technologies to give you the information you need at a specific level. Equation below can be used to account for some local effects, including ground roughness. This formulation allows the evaluation of wind speeds at altitudes other than the reference altitude, taking into account the effects of roughness.

$$u(h, Z_0) = u_{ref} \frac{\ln \left(\frac{h}{Z_0}\right)}{\ln \left(\frac{h_{ref}}{Z_0}\right)}$$

Wind speed data from the analysed sites are grouped and analysed as probability densities. The Weibull distribution function approximates the trend very well.

$$f(u) = \frac{k}{u}\left(\frac{u}{c}\right)^{k-1} e^{-\left(\frac{u}{c}\right)^{k}}$$

Where "k" represents the form factor and "c" represents the scale factor. In this way, the annual wind speed at the analysed location can be obtained with only two parameters. These parameters are calculated from the mean wind speed and standard deviation.

This function represents the probability that the wind will have a specific velocity range in a year. That is, it is expressed as a percentage based on 8760 hours per year.

Wind turbines use wind energy to generate electricity. In fact, they convert the kinetic energy of the wind into the mechanical energy of the rotor, which is then converted into electrical energy by the motor.

Wind force depends on the velocity and density given in the below equation.

$$P = \frac{1}{2}\rho A U^3$$

Where A represents area of the rotor blade.

From the equation we can observe that, the power is strongly dependent on the wind speed.

With current technology, it is impossible to convert all wind energy due to physical and technical limitations. Many theories explain the forces that wind rotors can produce. A dimensionless parameter is therefore provided that includes the various sources of loss and reduces the maximum power that can be drawn.

Betz theory specifies the maximum power that an ideal turbine can extract from the wind. According to this theory, the wind speed is undisturbed and two-dimensional, the rotor consists of an infinite number of blades, the density is constant, and there are no rotating waves. The dimensionless coefficient calculated from this theory is approximately equal to Cp, max = 0.59.

$$P = \text{Cp} \cdot \frac{1}{2}\rho AU^3$$

Wind turbine manufacturers should provide power curves for each generator. A power curve is a diagram that shows the power that can be drawn from a turbine at different wind speeds. Figure 1.10 shows an example of a power curve.
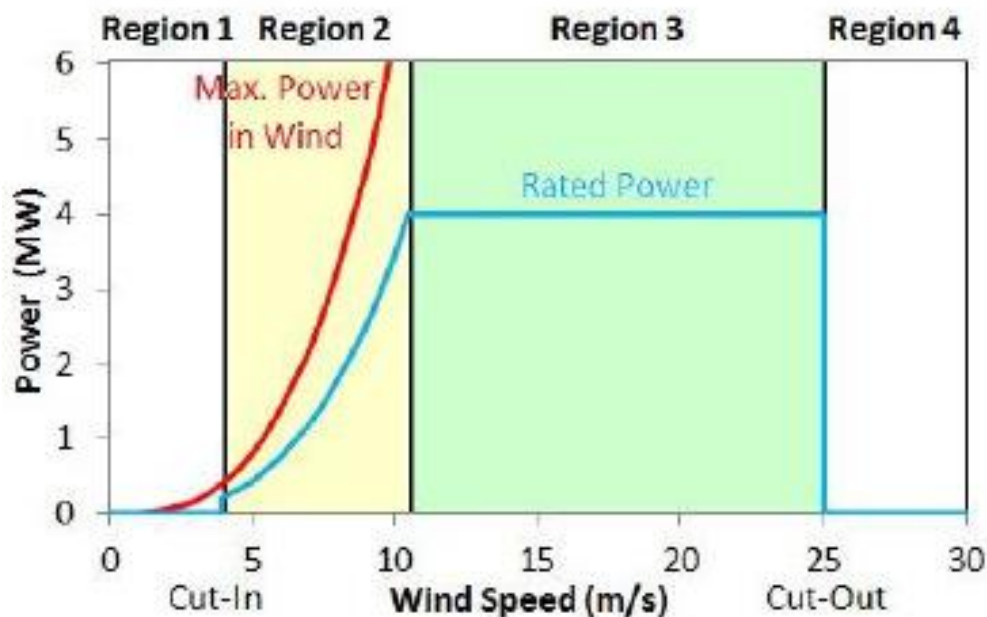
Figure 2-29 Power curve of wind turbine

As seen in regions 1 and 4, the wind speed is too low in the first region and too high in the fourth region, so the turbine cannot operate. In the latter case, it is desirable to activate the safety system as the turbine may experience structural problems. Area 2 generates more power as the wind speed increases. On the other hand, in region 3, the power remains constant.[10]

2.2 Calculation of energy production

Turbine productivity comes from the sum of the product of the wind frequency distribution and the generator output curve. The probability distribution should be used to take into account the time present in the year, and for the above reasons, slower than the cut-in speed and faster than the turbine cut-out speed is excluded from the calculation.

$$E_{AC}(kWh) = 8760 \sum_{u=u_{cut-in}}^{u=u_{cut-off}} \left(P_{el}(u) \cdot f(u) \right)$$
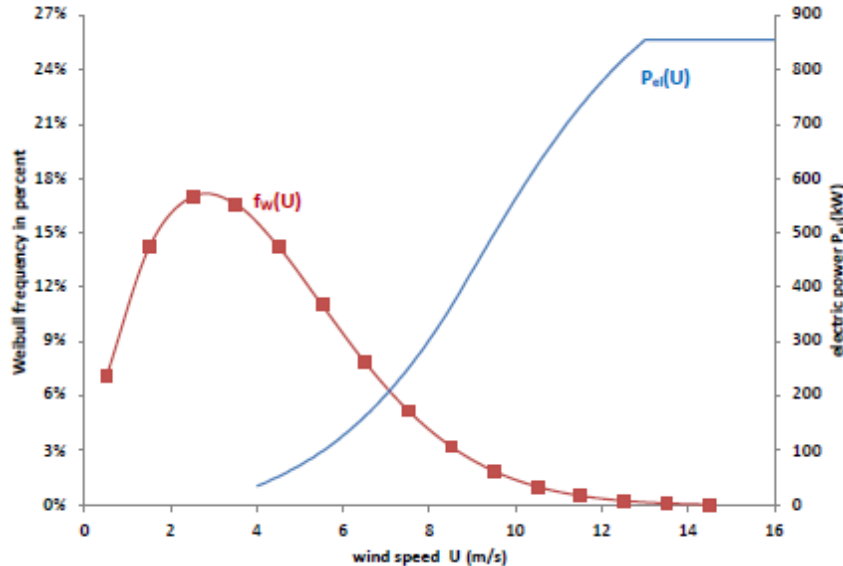
Figure 2-30 Power Curve and Weibull distribution

The productivity of the wind turbine when is calculated for the wind speed at the hub height.

2.3 Wind turbine components

Inside a wind turbine, a system is required that can convert the mechanical energy of the rotor blades into electrical energy. The first mechanism present in many commercial turbines is the gearbox, which can increase speed from 5-30 rpm to over 1000 rpm. Then there are motors that can convert mechanical energy into electrical energy. In addition, there are other systems within the turbine that can regulate the power of the turbine itself. For example, an adjustment system that allows the rotor axis to be adjusted based on wind speed and direction. The braking system can also control the most dangerous and extreme situations and finally bring the system to a halt. Figure shows the main components of the generator. Specifically for electromechanical generators has two different technologies. Fixed speed and variable speed. The latter is the most used on the market, about 60%. Among these technologies, DFIG (Double Fed Induction Generator) is the most used as it allows the turbine to operate over a wider range of wind speeds.[11]
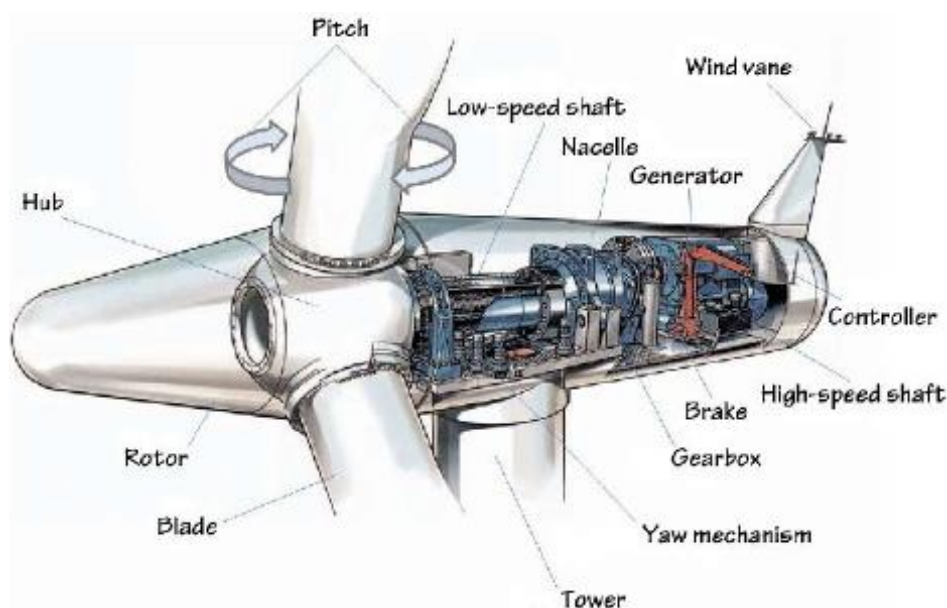
Figure 2-31 Components inside a wind turbine

2.4 Wind turbine classification & offshore technology

According to the IEC 61400-1 standard, turbines can be classified into seven major categories based on the average speed which measured at the hub, the standard deviation and two other parameters that consider the extreme speed measured.[11]

In recent history, offshore wind turbines are getting more and more attention. This configuration allows for large-scale wind farms and produces more production than onshore installations because wind propagation is largely unimpeded. In addition, this type of installation reduces the effects of noise pollution and landscape restrictions. However, it adds to the cost of installation and maintenance. From the 2019 IEA report on this source, the technical potential of electricity is estimated to be around 420 000 [TWh] per year worldwide, most of which should be installed in the very deep sea. In 2018, 2.4% of the European Union's electricity was produced by this type of offshore technology. Offshore wind turbine installations can be done using two different techniques: ground-based and floating. The latter is mainly used at sea depths of 50 m and above.[10]

3 Electrochemical storage systems

The electrochemical storage system makes it possible to store electrical energy with a high efficiency of about 70-80%. This type of technology is mainly used in electric vehicles and renewable energy power generation systems. The main drawbacks of these systems are their high installation costs and their low ability to store large amounts of energy. One of the main parameters used to characterize a battery is capacity. It is defined as the amount of energy that can be stored and is measured in [Ah]. Another very important parameter is the number of cycles. H. The number of charges and discharges that can be performed. For batteries connected to a renewable system, this is an important parameter for battery life. In fact, the system has several activations to ensure continuous load satisfaction.[13]

3.1 Principle of operation

An electrochemical cell is a system that directly converts chemical energy into electrical energy and vice versa. The main components of the electrochemical cell are two electrodes, an electrolyte, and a conductor for the flow of electrons. A battery is an electrochemical cell whose two electrodes are called the anode and cathode.

An oxidation reaction occurs at one of the electrodes, causing electrons to be emitted. At the other electrode, a reduction process occurs when the electrons recombine with the ions. The electrolyte material located between the two electrodes allows the passage of ions between the two electrodes and restricts the passage of electrons. Instead, the electrons travel through the outer conductor. These processes create a potential difference between the flow of electrons (currents) from the outer conductors and the oxidation and reduction processes that take place at the electrodes.

The figure shows a representative diagram of the battery charging and discharging process. Two processes are double. During the discharge phase, an external load can be powered, but during the charging process the process must be activated by an external source to cause the reverse reaction. This mechanism allows the battery to be charged when there is surplus power, stored in the battery

for a period of time, and discharged when external energy is needed. The energy is then stored in the battery in the form of chemical energy.[13]
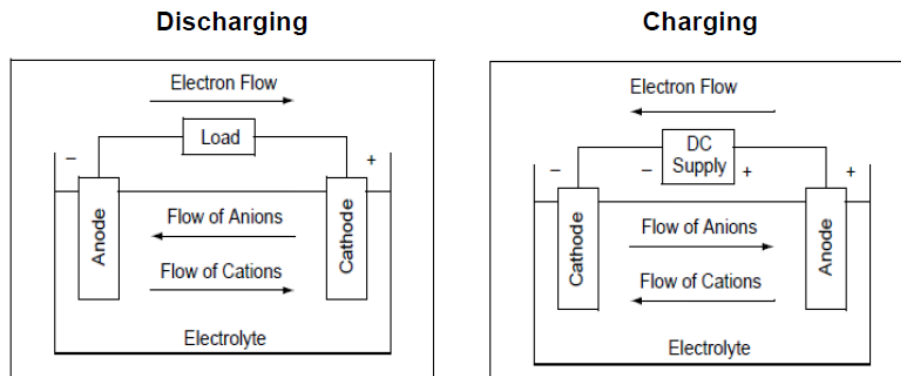
Figure 3-32 Charging and Discharging process of battery

3.2 Different battery technologies

Batteries are differentiated based on the materials used.

3.2.1 Lead-acid battery

$$Pb + PbO_2 + 2H_2SO_4 \leftrightarrow 2PbSO_4 + H_2O$$
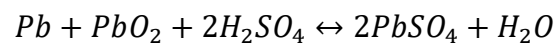
In this configuration, the anode is made of lead and the cathode is made of lead oxide, as shown in the figure.
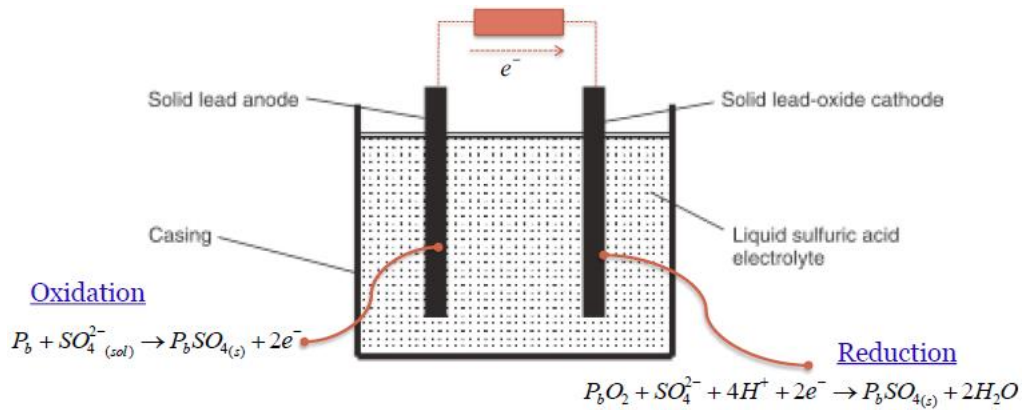
Figure 3-33 Lead Acid Battery

This type of technology is the most used on the market due to its performance and low cost. However, it has a shorter service life and requires lower energy density and larger dimensions for industrial use.

3.2.2 Li-ion battery

$$Li_{1-x}CoO_2 + C_6Li_x \leftrightarrow LiCoO_2 + 6C$$
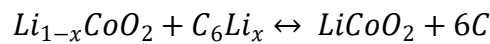
It has a high specific power and very fast charge and discharge times. However, they exhibit dangerous behaviour when exposed to high electrical or thermal overloads.

Table 2 Batteries in market

	Specific Energy [Wh/kg]	Energy Density [Wh/L]	Life cycle	Specific power [W/kg]
Lead Acid	20-35	54-95	≤800	250
Ni-Cd	40-50	70-90	≤1200	220
Ni-MH	70-95	150	≤1000	200-300
Li-ion	150			420

As mentioned earlier, lithium-ion batteries have a higher specific energy than lead-acid batteries, resulting in more compact and lightweight systems that are useful in a variety of applications.[13]

4 General aspects of planning & Introduction to the RES_tool program

In this thesis, the program "RES_tool" is used to perform planning analysis and to obtain estimates of key indicators which are used for energy and economic analysis. The program is implemented in Python software. This is done in a few functionalities where solar and wind system models have been implemented and estimates of some key parameters, which can be obtained during the design phase of a new RES project, as described in the following paragraphs. Below figure shows a simplified representation of the functions performed by the program. In this representation, the RES_tool program is represented as a "black box" into which the system's weather data, electrical load, economic and energy data are entered. Through it is possible to obtain the most important useful parameters for planning the analysis.[14]

Figure 4-34 RES tool[14]

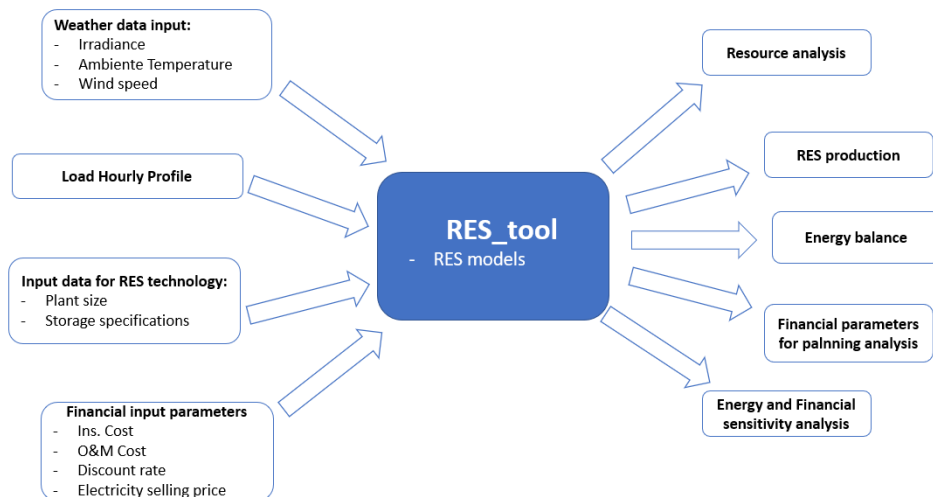To calculate various parameters, it is essential to import hourly weather data for each selected location. Meteorological data are downloaded from the PVGIS website. We download this data using API key in JSON format from the PVGIS website. And then with the help of Python codes this Data in JSON format is converted into data table.

From the PVGIS website we download the following data:

1. Irradiance which is expressed in [kW/m^2].
2. Ambient temperatue of air expressend in [°C].
3. Average wind speed at 10m height expressed in [m/s].

In this tool the data can be downloaded between the year 2005 to 2016. By entering the years in the appropriate entry box and the latitudes in their corresponding entry boxes, we can download the meteorological data from the PVGIS website. From this downloaded data we can calculate energy produced by the PV plant and wind farm.

The tool calculates the energy produced by the PV plant and wind farm for the number of years entered in the tool and the data for 25 years are replicated smartly by the tool based on the number of years entered by the user. And there are also other variables which are needed for energy calculation of solar and wind forms and these values are entered in default and the user can also change it according to his simulations.

If the user wants to simulate only Solar farm but not wind farm, it is possible by entering number of turbines equals 0 and vice versa.

Along with this meteorological data, the hourly load data is also required, and it should be provided by the user. The load data is provided as input in the excel format and this hourly load data can be entered in 2 different ways. First way is providing hourly data for the whole year and percentage of incremental of the hourly data for next 24 years and second way is by providing hourly load data for all the 25 years.

After importing the weather data, the imported data can be typically evaluated within the program. A "heat map" is created by summarizing the monthly average data for each year of temperature, solar radiation, and average wind speed. Standard deviation, variance, mean, and median data for the presented data are also

automatically provided. Through these tables, it is easy to perform an analysis of the appropriate site resources, taking into account the distribution of the amount to be considered.

The description of RES_tool, RES models are implemented to represent the working principles of these technologies. Within the program you can choose the size of the generator and the capacity of the battery. By choosing parameters, the program can calculate plant productivity, exchange with the grid, self-sufficiency and self-consumption values. It is also possible to define economic parameters for the plants, which are used by the program to calculate the economic parameters as described previously. In this case, it is advisable to correctly define the acquisition costs of photovoltaic systems, wind turbines and energy storage systems. In addition, the applicable annual maintenance costs and the discount rate applicable to investments in these projects should be defined. When calculating financial data, the sales price of energy must be defined. The existence of the following incentive systems is conceivable for these technologies. After defining these variables, the RES_tool program can automatically calculate the values of economic parameters such as NPV, PBT, LCOE and IRR.

This analysis is carried out for the number of years entered by the user and then replicated smartly by the tool for 25 years. The main feature of this thesis program is the sensitivity analysis this sensitivity analysis is carried out for both energy and economic analysis we observe the change in the sensitivity of the plants by changing the variables inserted by the user.

PV system	WT system	Storage system
Nominal Power	Number of Turbine	Storage capacity
	Type of the WTG	Max and min state of charge
		Charge and discharge efficiency

Table 3 Energy data that is possible to change for sensitivity analysis

PV system	WT system	Storage system
Installation cost	Installation cost	Installation cost
O&M	O&M	
Discount rate	Discount rate	
Electricity selling price	Electricity selling price	

Table 4 Financial data that is possible to change for sensitivity analysis

4.1 Description of UI of the application

4.1.1 Planning analysis

The main objective of this thesis is planning and analysis of development of renewable sources i.e., installation of PV and Wind power systems along with battery energy storage systems.

The tool analyses and calculates the optimal size of the PV and Wind systems such that it is profitable and self-sufficient.

The working procedure of the tool is explained briefly in the flow chart.
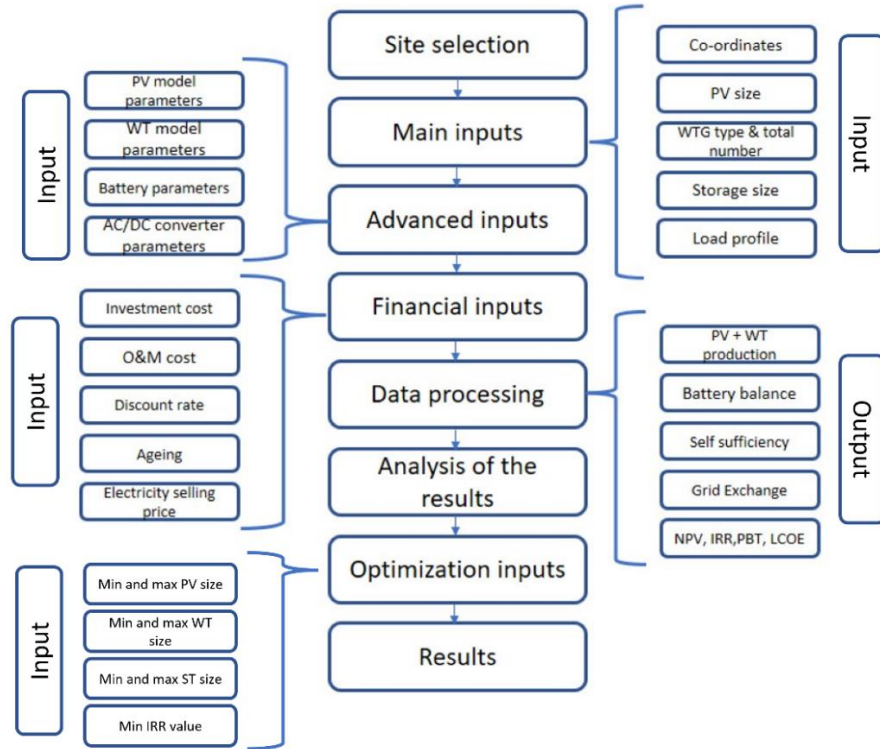
Figure 4-35 Flow chart

1. Site selection:

   Through the case study all the constraints such as pysical and territorial were analysed and the resouce availability was evaluated. Hence by this process we evaluated and identified suitable places for installation of power generators.

2. Main Inputs:

   To calculate the energy production of PV and wind sytems we need some of the main inputs such as Co-ordinates of the site so that tool can download all the necessary meteriological data from PV gis website. PV size that we are going to be installed. Then selection of type of the WTG and number of WTG for energy prodcution. Battery energy storage system size.and yearly load profiles. All these inputs are main inputs mandatory for the analysis.

3. Advanced Inputs:

   Along with the main inputs some of the advanced parameters of different components are also required for the analysis. These inputs are by default has values. If the user wants to change these values, he can do so by entering appropriate values.

4. Financial Inputs:

   To do the economic analysis tool needs some finacial parameters. Some of the main financial inputs are Investment cost, Operation and maintenece cost, discount rate provided by the government, selling price of the electricity.

5. Data processing:
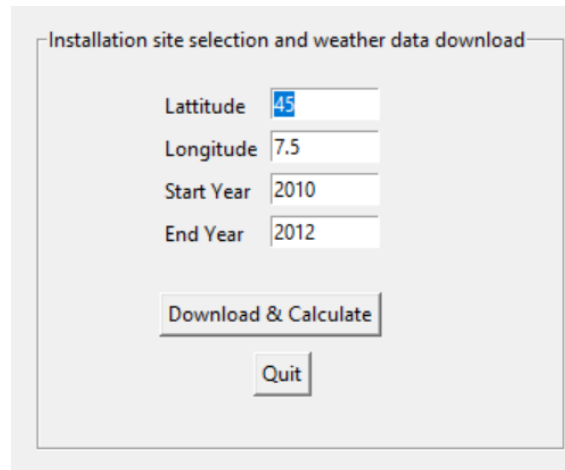
   By fetching all the above inputs the tool calculates the PV and Wind productivity along with the BESS. Then calculation of self sufficiency of the systems is calculated by the tool. And then the tool calculates all the financial parameters i.e. NPV, IRR, LCOE, PBT of the plant

6. Analysis of the reports:

   The results obtained in the above step is analysed to understand that the results obtained satisfy the pysical and economic constraints and are cosistent with the target.

7. Optimization inputs:

   The optimization of PV capacity, wind turbine capcity and BESS capcity is optimized to achive higher self sufficiency of the plant by contraining the IRR. Hence to perform this operation some inputs such as minimun and maximum size of the PV, WT plants and BESS capacity has to be inserted and Minimum value of the IRR has to be inserted to perform the optimization process.

8. Optimized results:

   The tool perform necessary calculation to optimize the results and provides the optimal PV size, WT size and BESS size to obtain optimum self sufficency and IRR.

4.1.2 Installation site selection and weather data input frame.

Figure 4-36 Site selection and weather data input frame

The application has the site selection input frame, where the user can insert the latitude and longitude coordinates along with the starting year and ending year for simulation data that has to be downloaded from PVGIS website. After entering all the inputs and when the user clicks on the download button, the application starts the simulation.

4.1.3 Nominal power of generators and storage input frame

Figure 4-37 Nominal power of generators and storage input frame

Then there is a nominal power of generators and storage input frame, in this frame the user can insert the nominal power of the PV plant and the number of turbines that are going to be installed in the wind farm and also selection of wind turbine generator is also made in this frame, from the list of wind turbine generators that are stored in the database and along with this the storage capacity of the battery storage system is also inserted by the user inside this frame.

4.1.4 Electrical load profile input frame

Figure 4-38 Electrical load profile input frame

The application has the electrical load input frame, in this frame the user can load the excel file in which we have the data of the electrical load for the whole year. The electrical load can be provided to the tool in 2 different ways. The first

method is to provide the annual electrical load for each hour and annual increment percentage of the load Shown in the below figure.

	A	B	C
1	Hours	kW	% Increase
2	1-1-18 0.00	26278	0
3	1-1-18 1.00	23878	1
4	1-1-18 2.00	24817	1
5	1-1-18 3.00	24440	1
6	1-1-18 4.00	24007	1
7	1-1-18 5.00	25131	1
8	1-1-18 6.00	24407	1
9	1-1-18 7.00	28412	1
10	1-1-18 8.00	28931	1
11	1-1-18 9.00	28131	1
12	1-1-18 10.00	25557	1
13	1-1-18 11.00	24464	1
14	1-1-18 12.00	28973	1
15	1-1-18 13.00	29347	1
16	1-1-18 14.00	29765	1
17	1-1-18 15.00	29796	1
18	1-1-18 16.00	29384	1
19	1-1-18 17.00	25841	1
20	1-1-18 18.00	24390	1
21	1-1-18 19.00	29386	1
22	1-1-18 20.00	29730	1
23	1-1-18 21.00	29562	1
24	1-1-18 22.00	29793	1
25	1-1-18 23.00	29253	1
26	2-1-18 0.00	25921	1
27	2-1-18 1.00	24498	

Figure 4-39 Electrical load of 1st year and annual incremental percentage

For the load of type with one year data an incremental percentage is provided in the above format, the excel file should contain, 3 columns with the same name as shown in the above figure.

Figure 4-40 Electrical load for 25 years

For the second type the excel file should contain the hourly data of the electrical load for 25 years as shown in the above figure.

4.1.5 Peak shaving input frame

Figure 4-41 Peak shaving input frame

Along with the above inputs the user can also perform peak shaving for the plants and this peak shaving can be of 2 types and the first one is "limitation on maximum generated power" and the second one is "limitation on maximum power

injection". The corresponding input values for both the type of peak shaving is inserted by the user. If the user doesn't want to do any peak shaving no limitation option can be selected by the user.

These are the main inputs which are mandatory for performing simulation analysis of PV and wind farms along with the storage system.

4.1.6 Advanced inputs and parameters of PV conversion model

Figure 4-42 Advanced inputs and parameters of PV conversion model

Along with the main inputs the user can also insert advanced inputs which are necessary for calculation and simulation of energy analysis of PV plant. In the above figure we can observe the different losses that are present in the PV plant and these values are pre inserted in the tool and if the user wants to change it , can enter the desired values.
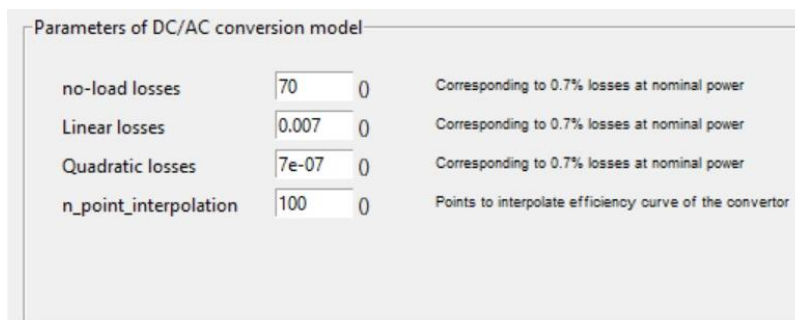
4.1.7 Advanced input parameters of winter turbine plants

Figure 4-43 Advanced input parameters of winter turbine plants

The application also have the advanced input frame for wind turbine plants, If the user wants to change the values shown in the above figure, can enter the desired values and run the simulation.

4.1.8 Advanced input parameters of an inverter
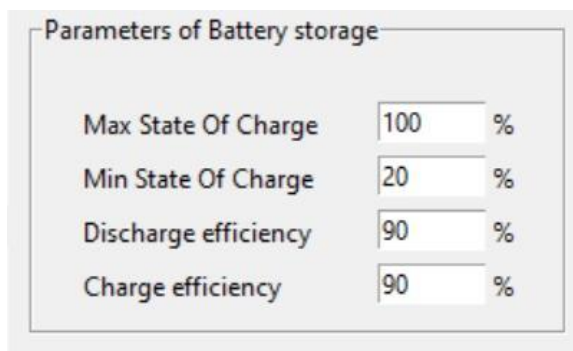
Figure 4-44 Advanced input parameters of an inverter

The values of different types of losses in inverter are inserted as show in the above figure, the user can change these values as per the type of the inverter is going to be installed for the plant.

4.1.9 Advance input parameters of battery storage

Figure 4-45 Advance input parameters of battery storage

The maximum and minimum state of charge of the battery storage system and discharge efficiency and charge efficiency of the battery storage system is provided by the user in this frame.

Once all these main inputs and advance inputs are provided by the user he can run the simulation by clicking on "Calculate" button. once the simulation is started the tool performs necessary operations for the energy and economic analysis of the plants and provides the results of the simulation.

4.2 Results

4.2.1 Results of first year

Results of First year		
PV productivity	MWh/MW/year	1327
Annual PV production	MWh/year	13270
Productivity of PV with Peak shaving	MWh/MW/year	1327
Annual PV production with Peak shaving	MWh/year	13265
WT productivity	MWh/MW/year	256
Annual WT production	MWh/year	5120
Productivity of WT with Peak shaving	MWh/MW/year	256
Annual WT production with peak shaving	MWh/year	5120
Discharged Energy	MWh/year	0
Charged Energy	MWh/year	0
Self Consumption	%	100%
Self Sufficiency	%	6%
Absorption from the grid / load	%	94%
Injection in the grid / load	%	0%
Annual Load	MWh/year	314326
MWh		

Figure 4-46 Results of first year

When the simulation is made to run, it does all the necessary calculations needed for energy analysis and economic analysis. The result of the first year of the energy analysis is listed in a table as displayed in the above picture.

4.2.2 Solar irradiance, wind speed and ambient temperature data

The hourly data of solar irradiance, wind speed and air temperature data are downloaded from the PVGis website.

	2006	2007	2008	2009	2010	2011	2012	2013	2014	2015	2016
Dec	204.61	184.02	208.43	179.24	174.84	194.26	205.75	210.88	180.65	192.01	188.55
Nov	149.61	198.71	174.24	167.29	150.13	170.57	203.30	187.27	180.88	142.32	193.83
Oct	149.46	177.11	174.61	202.26	179.59	196.89	179.99	184.56	181.83	204.04	179.29
Sep	143.93	155.61	184.49	162.12	159.86	172.63	178.45	163.49	175.44	181.70	143.54
August	139.23	148.75	156.88	169.24	145.74	149.65	155.46	160.45	152.07	171.68	143.46
July	136.56	139.55	152.88	146.16	138.64	149.04	161.84	142.49	154.29	166.72	118.21
June	130.37	139.15	148.17	168.06	150.66	138.15	156.66	143.15	172.64	156.96	120.61
May	159.91	191.47	195.85	183.67	191.31	195.63	196.34	185.18	186.69	174.88	167.19
April	191.72	212.33	209.41	202.92	201.75	201.66	195.08	200.75	205.22	195.17	200.78
March	206.44	235.53	201.72	224.04	229.01	236.90	235.20	221.65	229.09	225.03	216.50
Feb	211.16	211.40	191.90	217.00	208.17	207.91	220.35	200.29	197.73	213.42	193.20
Jan	207.84	216.95	218.68	221.77	210.70	220.74	222.36	225.95	219.84	210.22	197.73

Total Yearly Global irradiance (kW/m2)

Figure 4-47 Global irradiation heatmap

The sum of global irradiation off every hour for the month is plotted as a heat map. And from this graph, user can analyse the months in which the solar irradiance is high and the months in which solar irradiance is low. This helps in proper planning of PV plants

68

Figure 4-48 Avg wind speed

Average wind speed for each month is plotted as a heat map as shown in the above figure. With the help of this graph, planning of wind farm can be made easier. User can observe the months in which, wind speed is high and months in which wind speed is low. This graph also helps in selection of type of wind turbine generator.

4.2.3 PV + WT generation vs Load
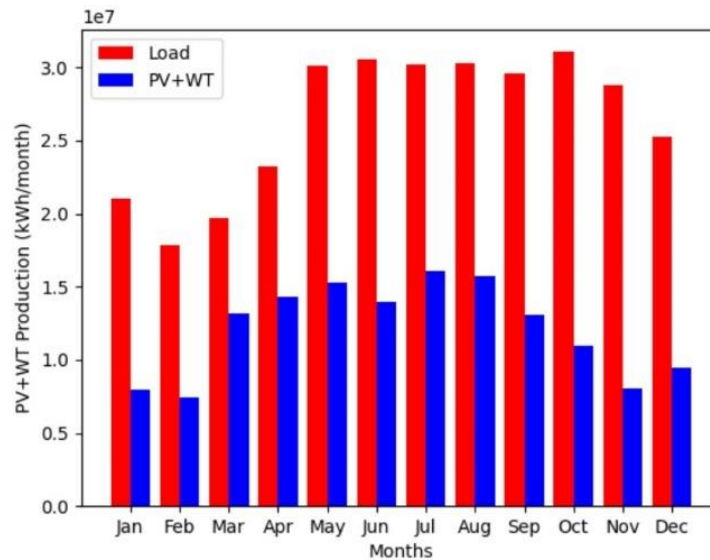
Figure 4-49 Production vs Load

Average production of wind turbine plus PV plant is compared with the average load needed for each month. From this graph user can analyse if the plant is oversized or undersized. If the load is higher than the PV + WT production, then the plant is undersized and if load is lesser than the PV + WT production then the plant is oversized. In the above figure we can conclude that the plant is undersized, and it doesn't satisfy the load.

4.2.4 Daily production results(Graph)
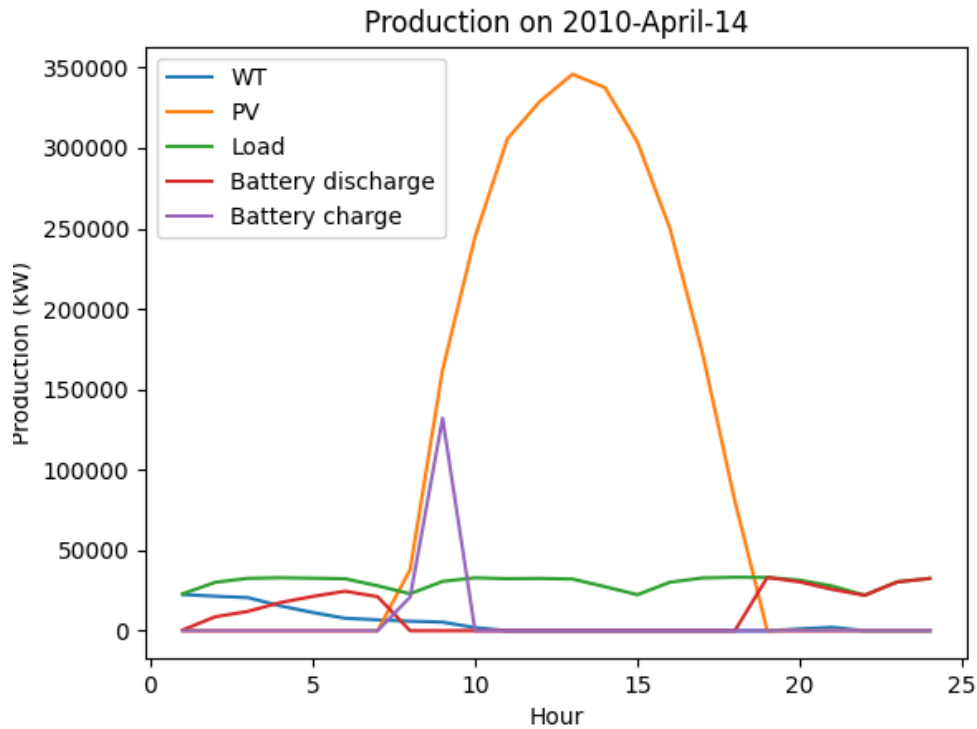
Figure 4-50 Production results, Single day

The energy produced by the PV plant and the wind turbine is plotted as a graph along with load required and battery charge, discharge values off each day. From this graph, user can analyse the production of each day, and charging and discharging of battery, thereby predicting, if the plant is able to satisfy the load, or the plant has to absorb energy form the grid.

4.2.5 Monthly production results (Graph)
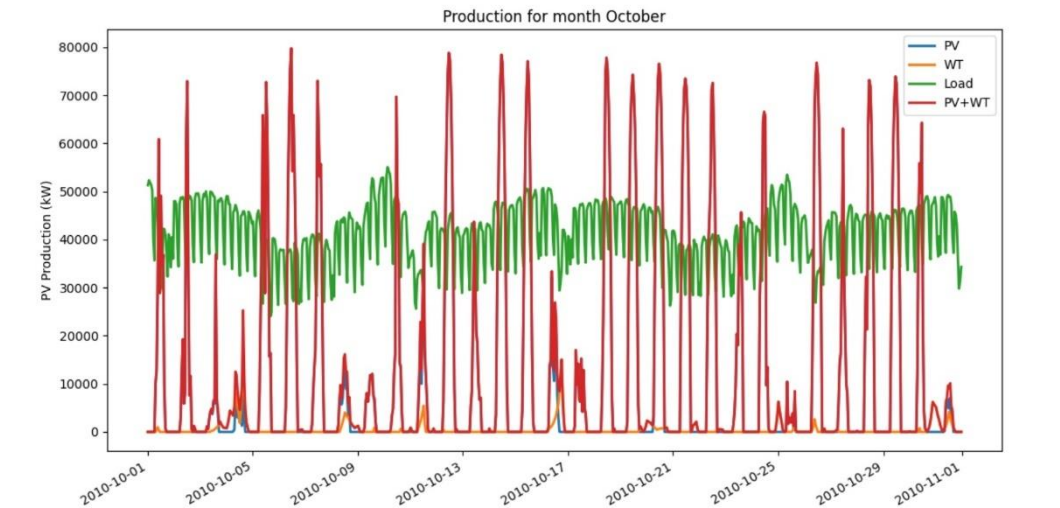
Figure 4-51 Monthly production results

Energy production by PV plant and wind turbines for each day of the selected month is plotted as a graph as shown in the above figure.

4.2.6 PV production vs Wind turbine production
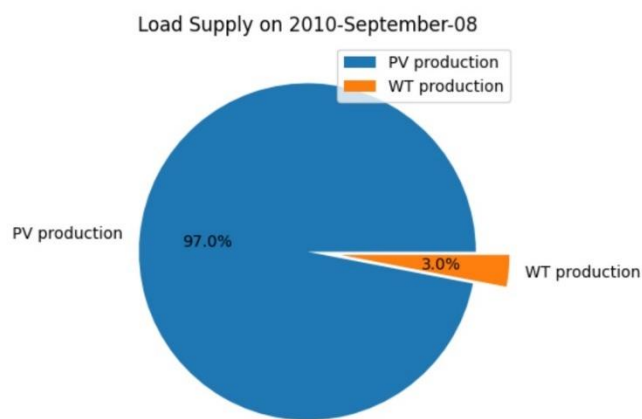
Figure 4-52 PV vs WT production

The daily PV production and wind turbine production is calculated and plotted in the form of pie graph as shown above.

4.2.7 Grid Exchange
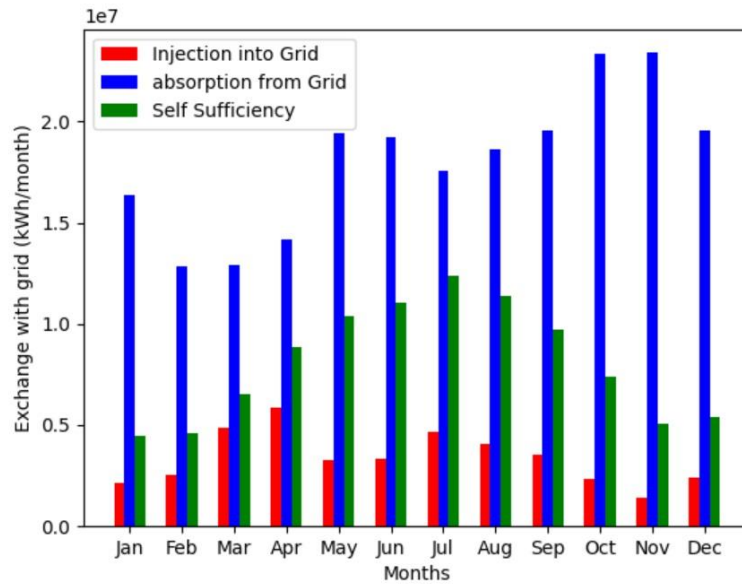
Figure 4-53 Average grid exchange

The monthly average of energy absorption from the grid energy injection to the grid and the self-sufficiency of the plant is plotted as bar graph and is shown in the above picture.

4.2.8 Daily grid exchange
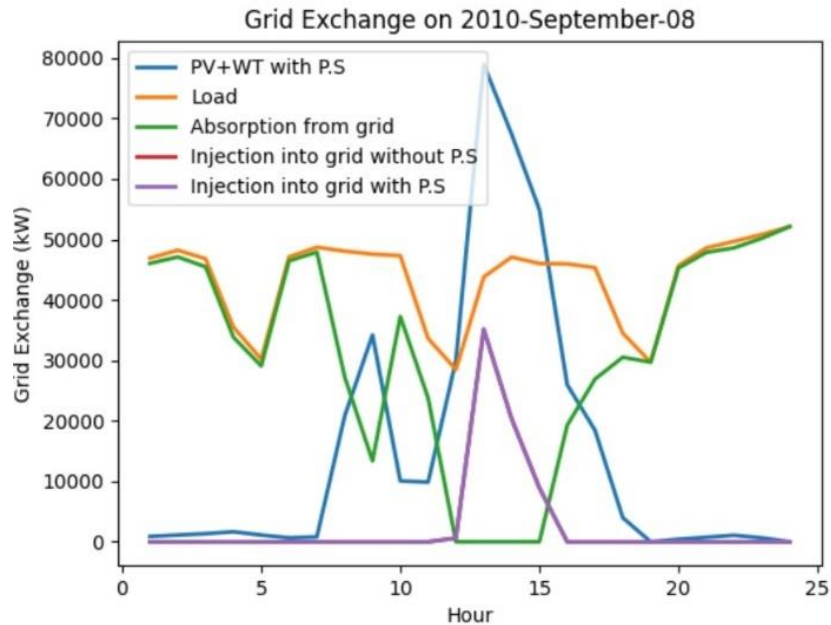
Figure 4-54 Daily grid exchange

The daily electricity exchange with grid is calculated and plotted as bar graph as shown in the above figure. From this graph user can analyse the grid exchange values, such as injection into grid and absorption of electricity from the grid. From the above graph it is visible that up to 7:00 a.m., there is no production of electricity from the PV plant and from the WT plant. Hence, to satisfy the load, the plant absorbs electricity from the grid. Once the production satisfies the load, the excess od electricity is injected into the grid.

4.2.9 Monthly grid exchange
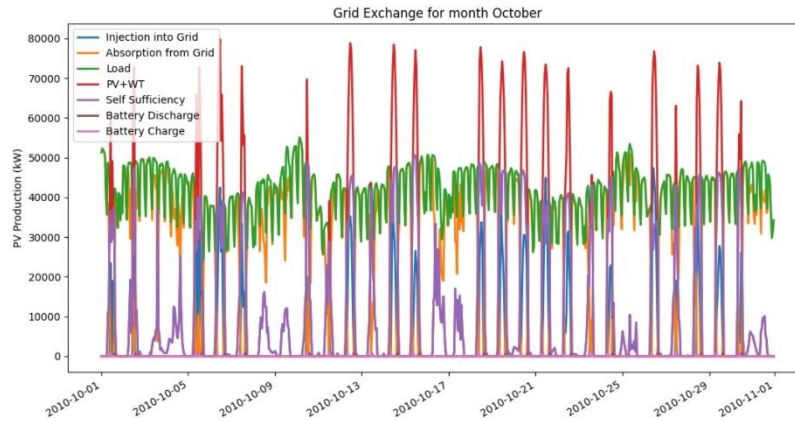
Figure 4-55 Monthly grid exchange

The monthly electricity exchange with the grid for each day is calculated and floated as bar graph as shown in the above figure.

4.2.10 Monthly energy flow table

Energy flow of each month of year 2010(MWh/month)

	PV	WT	PV+WT	Load	Absorption f	Injection into	Grid Exch
Jan	6215.81	388.73	6604.54	20849.24	16368.94	2120.54	18489.48
Feb	6519.84	673.94	7193.79	17476.89	12844.64	2558.47	15403.1
Mar	10764.65	645.64	11410.29	19482.64	12928.53	4850.93	17779.46
Apr	14263.4	476.68	14740.08	23036.78	14165.32	5863.56	20028.88
May	13115.63	539.39	13655.02	29788.28	19398.51	3259.34	22657.85
Jun	14066.53	378.44	14444.97	30284.56	19212.35	3368.2	22580.55
jul	16767.51	266.85	17034.35	29932.2	17566.67	4663.42	22230.09
Aug	15008.38	431.61	15439.99	29954.69	18600.12	4079.34	22679.46
Sep	12928.19	299.46	13227.65	29287.25	19574.23	3509.57	23083.79
Oct	9349.25	371.84	9721.09	30756.27	23373.77	2334.37	25708.14
Nov	6037.61	450.92	6488.53	28498.87	23402.28	1389.33	24791.61
Dec	7615.56	196.23	7811.79	24978.79	19568.62	2397.94	21966.57

Figure 4-56 Monthly Energy flow table

The monthly energy production of PV plant and wind turbine is calculated, and they are listed in the table along with the required load values and grid exchange values such as Injection of electricity into the grid and absorption of electricity from the grid finally the self-sufficiency of the plant.

4.2.11 Daily energy flow and energy balance table

Energy Flows(AC)	kWh/day
PV Production	534611
WT Production	705
PV+WT(With peak shaving)	535316
LOAD	1036215
Battery Discharge	720
Battery Charge	889
Absoprtion from grid	655150
Injection into grid	154082
Grid Exchange	809233
Self sufficiency	381065

Energy flow on 2010-October-14

Energy Balance	
Absorption from the grid/load	63%
Injection in the grid/load	15%
Production from renewables / loa	52%
Self-sufficiency with respsect to lc	37%
Absorption from the grid/generat	122%
Injection in the grid/generation	29%
Self-sufficiency with respect to ge	71%

Energy Balance on 2010-October-14

Figure 4-57 Daily energy flow and energy balance table

The daily energy production of PV plant and wind turbine is calculated, and they are listed in the table along with the required load values and grid exchange values such as Injection of electricity into the grid and absorption of electricity from the grid finally the self-sufficiency of the plant. And also, the battery exchange value such as battery discharge and bracket charge are also listed in the table. Along with this daily energy balance table is also listed for the selected date.

4.2.12 Wind turbine selection.

Years	Gamesa G114-	VESTAS V 150 - 4.0	VESTAS V 90 :	0	LTW77 800_kW IIA/IIIA	Vestas V90-2000_kW I	ENERCON E-82 E-2 IIA	Nordex N117
1.0	255.99	254.41	72.87		228.07	104.5	144.72	217.78
2.0	202.3	202.26	59.72		180.85	85.27	119.21	172.92
3.0	147.37	145.95	42.58		129.3	61.32	88.0	124.7
4.0	252.15	250.59	71.78		224.65	102.94	142.54	214.51
5.0	199.25	199.21	58.82		178.12	83.98	117.41	170.31
6.0	145.13	143.74	41.93		127.34	60.39	86.67	122.81
7.0	248.31	246.77	70.69		221.23	101.37	140.37	211.25
8.0	196.2	196.16	57.92		175.4	82.7	115.61	167.71
9.0	142.9	141.53	41.29		125.38	59.46	85.33	120.92
10.0	244.47	242.96	69.59		217.81	99.8	138.2	207.98
11.0	193.15	193.11	57.02		172.67	81.41	113.81	165.1
12.0	140.67	139.32	40.64		123.43	58.53	84.0	119.03
13.0	240.63	239.14	68.5		214.39	98.23	136.03	204.71
14.0	190.1	190.06	56.12		169.95	80.13	112.02	162.49
15.0	138.43	137.11	40.0		121.47	57.6	82.67	117.14
16.0	236.79	235.33	67.41		210.97	96.67	133.86	201.45
17.0	187.05	187.01	55.21		167.22	78.84	110.22	159.89
18.0	136.2	134.9	39.35		119.51	56.67	81.33	115.25
19.0	232.95	231.51	66.32		207.54	95.1	131.69	198.18
20.0	184.0	183.96	54.31		164.49	77.56	108.42	157.28
21.0	133.97	132.68	38.71		117.55	55.74	80.0	113.36
22.0	229.11	227.69	65.22		204.12	93.53	129.52	194.91
23.0	180.95	180.91	53.41		161.77	76.27	106.63	154.67
24.0	131.74	130.47	38.06		115.59	54.81	78.67	111.47
25.0	225.27	223.88	64.13		200.7	91.96	127.35	191.65

……

Figure 4-58 All wind turbine production data table

The calculation of wind turbine production is based on the wind speed data that we obtained from the PVgis website. This data for every time step is used for the calculation of production of each wind turbine production. The application calculates the wind turbine production of all the 10 wind turbines using appropriate formula and they are listed in table as shown in the above figure. From the above table we can select the WTG which has higher productivity.

4.3 Financial analysis

4.3.1 PV financial assessment

Figure 4-59 PV financial assessment

In this table we provide the investment cost, operation and maintenance cost, discount rate, degradation percentage of each year and electricity selling price. The other values such as total electricity production, Specific production, total electricity injection into the grid are calculated and displayed by the tool in the above table. These values are used for the calculation of financial assessment of the PV plant and wind farm.

4.3.2 Wind turbine financial assessment

Figure 4-60 Wind turbine financial assessment

Similar to PV in wind turbine financial assessment we provide inputs such as investment cost, operation and maintenance cost, discount rate, ageing degradation percentage of the plant for each year and electricity selling price. And values such as total electricity production, total grid injection and specific production are calculated by the tool and all these values are used for the calculation of financial assessment of wind turbine farm.

4.3.3 Storage financial assessment

Figure 4-61 Storage financial assessment

In the storage financial assessment table, we provide only one input that is investment cost, and this value helps in the financial assessment of the storage system.

4.3.4 Self-consumption

Figure 4-62 Self consumption

In this table we provide input that is value of the electricity consumed by the plant and the self-consumed electricity by the PV plant and the wind turbine farm are calculated by the tool and are displayed in the above table.

4.3.5 Tax reduction

Figure 4-63 Tax reduction

In this table we provide information regarding to tax reduction as the percentage of investment of the plant. Here we provide tax deduction value and also the validity of this tax reduction for both the PV plant and the wind turbine farm.

4.3.6 Output of financial assessment

Figure 4-64 Output of financial assessment

After getting all the necessary inputs for the calculation of financial assessment the tool calculates the internal return rate(IRR), net present value(NPV), total payback time(PBT) and levelized cost of energy(LCOE) of the plant by using appropriate formulas and these values are displayed in the above table.

4.3.7 NPV graph
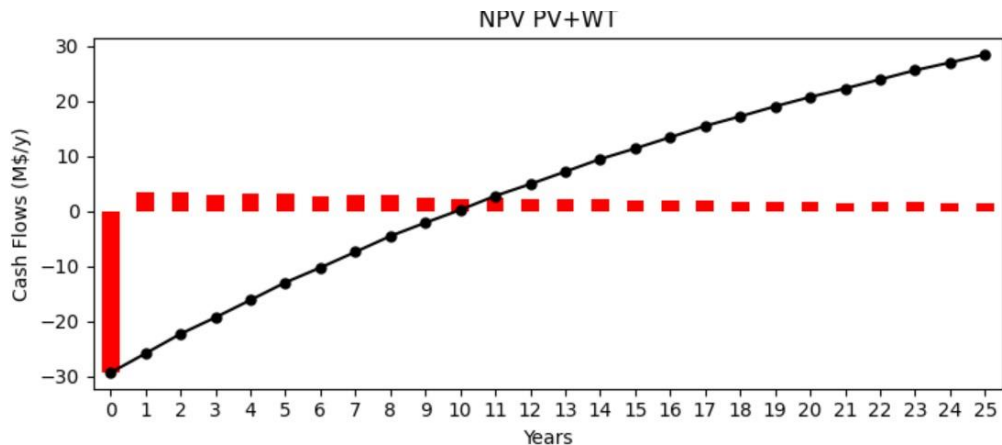
Figure 4-65 NPV graph

By using all the necessary formulas, the net present value of the RES plant is calculated, and the above graph was plotted by the tool using those calculated values and shown to the user.

5 RES Model

The basic fundamentals of solar and wind farms were discussed before. this section, describes about how these technologies are modelled inside this RES tool and the basic parameters that describes them.
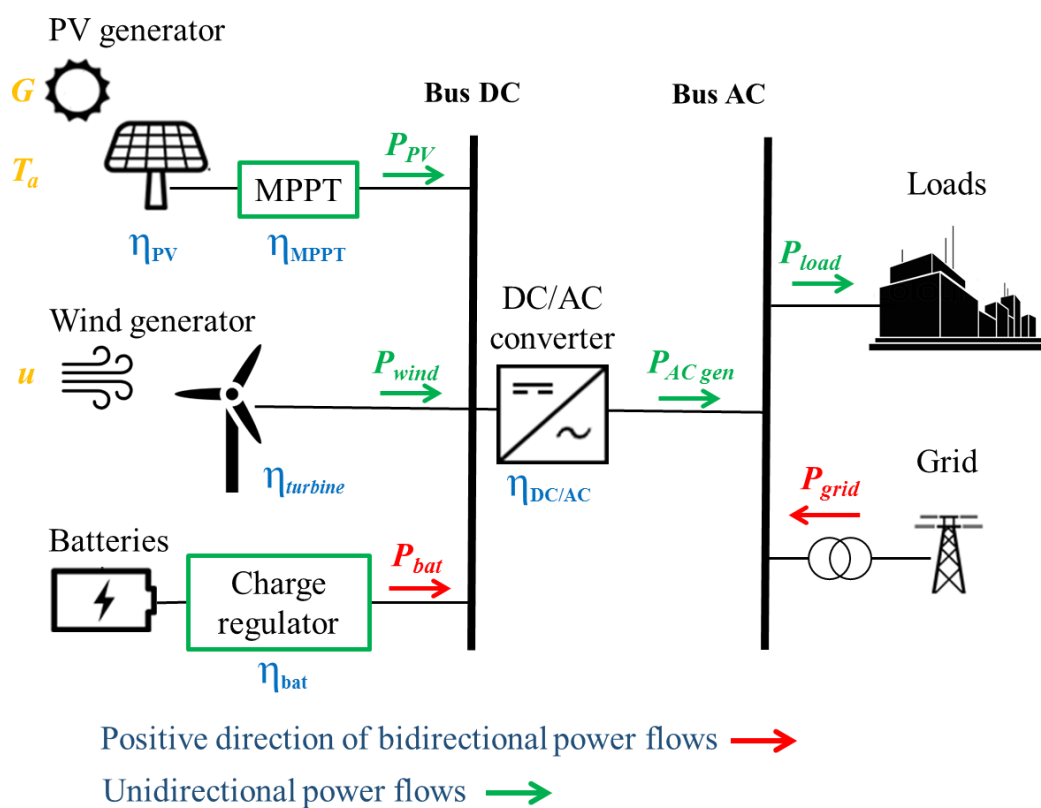
Figure 5-66 Representational diagram of the generation system[14]

Instead, the load is represented by the end user and the power grid, which has a generator connected and runs on alternating current (AC). For ease of analysis, AC nodes are also connected to a single DC node. Therefore, a converter capable of converting direct current to alternating current must be installed between the two nodes. Also, the inverter was supposed to be unidirectional, so it cannot draw energy from the grid to charge the battery. The inverter is sized for solar and wind

turbine generator power, while the battery only works in the absence of energy production from renewable energy generators.

5.1 Photovoltaic model

The formulas explained below are used to model the PV system with the RES_tool. From climatic data, it is possible to calculate the energy produced by these PV plants using several parameters that consider the actual conditions of use and operation of these systems.

$$P_{DC} = P_{PV} \cdot \frac{G}{G_{STC}} \eta_{mix} \eta_{th} \qquad (5.1)$$

$$\eta_{th} = 1 + \gamma_{th} * (T_m - T_{STC}) \qquad (5.2)$$

$$\eta_{mix} = \eta_{dirt} \cdot \eta_{refle} \cdot \eta_{mis} \cdot \eta_{cable} \cdot \eta_{MPPT} \cdot \eta_{shade} \qquad (5.3)$$

$$T_c = T_{air} \cdot \frac{NOCT - 20 \ [°C]}{G_{NOCT}} \cdot G \qquad (5.4)$$

Using the peak power rating P_{PV} measured at standard conditions (GSTC = 1 kW/m^2 and TSTC = 25 °C), calculates the dc power (equation 5.1). The G/G_{STC} ratio is used to account for irradiance effects in power calculations.

Losses can be divided into two categories: temperature dependent (equation 5.2) and temperature independent (equation 5.3).

As mentioned earlier, the simulation runs hourly, so the power drawn from the generator depends on the climatic conditions during the analysis period, with varying solar radiation and temperature.

As explained previously, PV module performance is affected by temperature. Especially as the cell temperature increases, the efficiency of the module decreases. Correct estimation of the cell temperature is recommended. For this we use the

NOCT model (equation 5.4). This calculates the cell temperature using irradiance and ambient temperature data obtained from PVGIS for the selected co-ordinates. This value depends on the type of installation and is indicated in the module's technical data sheet. For this analysis, a value of 45 °C was used for ground-mounted systems and a value of 47-48 °C for systems installed in buildings. In this case a semi-empirical formula is used to calculate the cell temperature Tc as a function of wind speed downloaded from the PVGIS site. Due to the enhanced phenomenon of convective heat exchange, when the wind speed increases, the cell temperature decreases at the same insolation and ambient temperature.

Table 5 Parameters used for modelling the photovoltaic system

$$P_{DC} = P_{PV} \cdot \frac{G}{G_{STC}} \eta_{mix} \eta_{th}$$

$$\eta_{mix} = \eta_{dirt} \cdot \eta_{refle} \cdot \eta_{mis} \cdot \eta_{cable} \cdot \eta_{MPPT} \cdot \eta_{shade}$$

Symbol	Value	Description
η_{dirt}	0,976	Caused by presence of dust and other materials on the surface. This value is lower for modules with a low inclination.
η_{refle}	0,973	Losses due to inevitable reflection phenomena that occurs on the glass of PV module
η_{mis}	0,97	This loss is caused by mismatch phenomena that occur when modules with different characteristic curves connected together
η_{cable}	0,99	Caused by dissipation of energy due to Joule effect due to the passage of current

		through the material of the cables $P_{diss} = R \cdot I^2$
η_{shade}	0,99	This loss depends on causes external to the generator & depend on the presence of the external protrusions that could reduce solar radiation which affects the PV module.
γ_{th}	-0,005 [1/°C]	
G_{lim}	0,0177 [kW/m²]	When solar irradiance is not high than the limit value it is impossible to activate inverter and therefore there is no electricity generation.

The PV module used in this study is fixed axis. The life of the plant is assumed to be 25 years and a correction factor of 0.5% per year is used to reduce the efficiency of the plant to account for plant aging effects.

5.2 Wind turbine model

The Modelling of wind turbine is done through the equations listed below.

$$P_{mec} = \frac{1}{2} \cdot \rho \cdot A \cdot U^3 \cdot C_p(\lambda, \beta) \qquad (5.5)$$

$$u(h, Z_0) = u_{ref} \frac{\ln(\frac{h}{Z_0})}{\ln(\frac{h_{ref}}{Z_0})} \qquad (5.6)$$

With equation 5.5 we can calculate the DC power produced by a wind turbine. However, this parameter highly depends on the power factor, which is a function of tip speed ratio (λ) and blade inclination (β). This parameter is often calculated from experimental testing of generators.

We calculate productivity using performance curves provided by each wind turbine manufacturer. In this curve, the active power produced by the turbine is related to different wind speeds and hub heights.

Within the RES_tool program there are power curves for 10 different turbines. Below figure shows curves for some existing turbines. All the selected turbine is horizontal axis type.
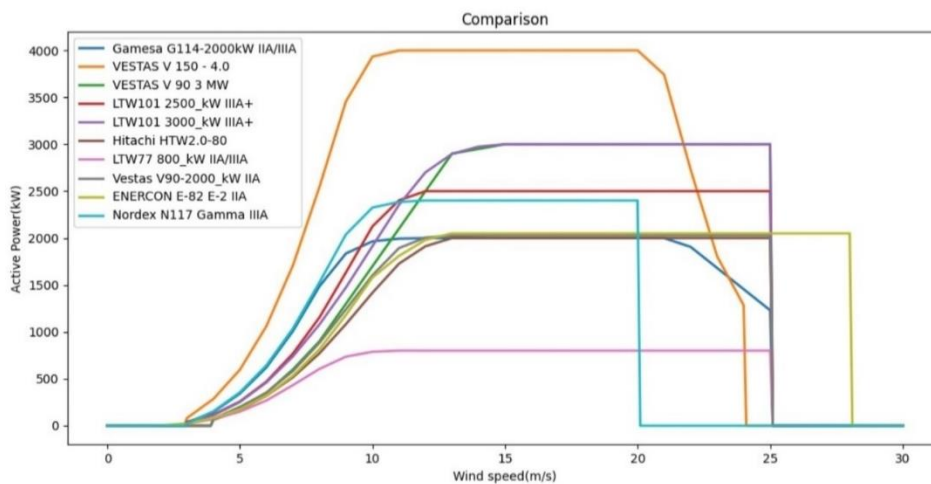
Figure 5-67 Power curve of all WTG

As discussed before, we can distinguish four distinct regions of different operating speeds within the performance curve. From above figure we can see how the active power of the turbine becomes zero when the wind speed is higher than the limit speed that the turbine can withstand, but it is clear that different turbines have different operating ranges and therefore can operate under different conditions. The curve shown in above figure is the result of linear interpolation of information provided by suppliers.

Meteorological data that obtained from PVGIS sites are referenced to an altitude of 10 [m]. Manufacturer data on generator power output is referenced to hub height, so weather data related to hub height must be obtained in order to be able to use the power curve correctly. Equation 5.6 is used for this purpose. A value of 0.15 [m] was chosen for the roughness length in this work.

As discussed before, wind turbine productivity is calculated using data from power curve and wind distribution. The Weibull distribution was not used in this

study, but the distribution was calculated experimentally. Hourly wind speed data can be obtained from the PVGIS site. They are arranged in a Cartesian coordinate system showing the wind speed value and the number of hours in the year when this value was measured. The distance between one velocity value and the next is 0.5 m/s. In this way, the velocity distribution for one year is obtained. The velocity distribution obtained by this method and the power curve of the reference system are shown in below figure. In which method can productivity be calculated by adding the obtained values hourly.
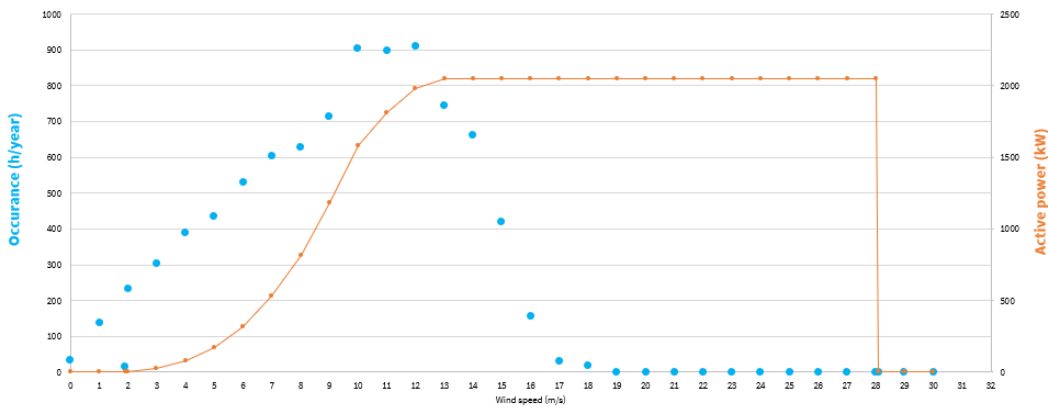
Figure 5-68 Distribution curve vs Power curve

The life of the plant is assumed to be 25 years and a correction factor of 0.5% per year is used to reduce the efficiency of the plant to account for plant aging effects.[16]

5.3 Model of the electrochemical storage in RES_tool

The most important indicators of electrochemical storage properties are charge capacity and state of charge (SOC). Capacities are defined in the product datasheet. Within the RES_tool program, this parameter can be changed based on the characteristics of the system to which the storage is attached. This work assumes that the storage system will be replaced every 10 years and that the maximum number of cycles per battery is 10,000. To model a storage system correctly, we need to define the state of charge. Defined by below equations.

$$SOC(t) = SOC(t-1) + \left(\frac{|P_{bat}| * \Delta t}{V_{bat} * C_{bat} * \eta_{bat,c}} \right) \qquad (5.7)$$

$$SOC(t) = SOC(t-1) - \eta_{bat,d} * \left(\frac{|P_{bat}|*\Delta t}{V_{bat}*C_{bat}} \right) \qquad (5.8)$$

by calculating these parameters, we are able to calculate the percentage of battery charge. Thereby we can estimate the amount of energy that can be used for discharging and amount of energy required to charge the battery fully. Equation 5.7 explains about the state of charge of the battery and equation 5.8 describes about the state of discharge of the battery. both these parameters have different efficiency values.

It is important to define the minimum state of charge of the battery and the maximum state of charge of the battery. In our thesis work we have assumed SOC_{min} equal to 20% and SOC_{max} equal to 100%

The SOC (t) value is a function of the previously calculated value and also depends on charge or discharge efficiency and nominal energy value. As can be seen from equations 5.7 and 5.8, the SOC depends on the average power consumption or the consumption at a particular point in time multiplied by the point in time under consideration.

$$SOC(t) = SOC(t-1) + \left(\frac{|P_{bat}|*\Delta t}{V_{bat}*C_{bat}*\eta_{bat,c}} \right) \qquad SOC(t) = SOC(t-1) - \eta_{bat,d} * \left(\frac{|P_{bat}|*\Delta t}{V_{bat}*C_{bat}} \right)$$

Quantity	Value	Description
Total capacity of storage	*Selected value [MWh]	This capacity ndicates how much electric current the battery can deliver in a given instant of time
SOCmin	20 [%]	This value refers to the nominal capacity and is expressed as percentage. The battery must not be

		discharged if reaches the minimum value.
SOCmax	100 [%]	It is not possible to charge the battery beyond its max storage limit
$\eta_{discharge}$	100 [%]	In this case an ideal discharge process is assumed, in reality this value is different from 100%
η_{charge}	90 [%]	Not all energy is stored perfectly, and a certain amount is dissipated during the process as heat
Max number of cycle	10 000 [-]	Maximum num of charge – discharge cycles from datasheet
Maximum lifetime	10 [years]	Max number of the years from datasheet of the storage

Table 6 BESS parameters

5.4 DC / AC converter model

It is nothing but an inverter which converts DC current into AC current. The working principle of this DC/AC converter has been discussed previously. The working of the DC AC converter is explained below paragraph.

$$\eta_{inv} = \frac{P_{AC}}{P_{DC}} = \frac{P_{DC} - P_{loss}}{P_{DC}} \tag{5.9}$$

$$P_{loss} = P_0 + C_L \cdot P_{DC} + C_Q P_{DC}^2 \qquad (5.10)$$

The inverter efficiency is defined as the ratio of output AC power to the input DC power. Through the semiempirical formula we calculate the losses. P_0 is losses appear when we don't have any conversion in progress. C_L and C_Q Corresponds to the linear and quadratic loss coefficients which appear due to the presence of diodes and resistors.[9]

6 RES installation in India

The economic development of the country is measured by its energy demand of the economy. Current estimates have predicted that demand for basic energy sources is set to increase in coming decades. According to the reports the energy demand in India is set to increase by 200% by 2040. To overcome this steep rise in energy demand, India has to increase its energy production sources.

With the global trend India has also shifted towards renewable energy sources to meet its demands. India is tropical country which has huge resource of solar energy.

6.1 Energy context in India

In India energy sector was majorly operated using coal as fuel source. The electrical capacity in India is 160GW in 2018. The Government of India has set up the Additional Energy Sources Commission in the Ministry of Science and Technology to promote research and development in the solar power sector.[15]

Lack of use of available non-traditional resources led to the formation of many policies that later shaped development solar industry. Solar energy accounts for 19% of all installed renewable energy. Positive trends in solar installation and development helped the government of India to invest INR 30000 million in RES (equivalent to 30 billion) and will be offered exclusively. Solar power in India targets 100 GW by 2022.[15]

6.2 Selection of suitable site in Karnataka, India.

In this thesis work we mainly concentrate on installation of onshore wind generators and photovoltaic systems for the region of Karnataka in India. Karnataka is a state in southwest India with Arabian Sea coastlines. Karnataka has a population of about 64 million inhabitants with energy consumption of 61,131 GWh yearly.

6.2.1 Territorial constraints

Many fields in the region of Karnataka are liable to be subjected landscape restraints, and it contains many forests which are reserved, to maintain the vegetation and animal.

According to international standards, wind turbines should be installed at least 100m away from the road network. However, choosing a location that is too far from the road network (>2000m) can be inconvenient. Both construction and maintenance work on facilities can present various difficulties in reaching the chosen location.

Proximity to city centres is advantageous in reducing transmission losses in the grid, but it also poses various problems for both solar and wind farms. In a photovoltaic system, the presence of many obstacles can increase the number of shadows and the loss of generated energy. For wind turbines, wind turbulence levels increase closer to city centres, which can lead to production losses and safety issues. In addition, the presence of wind turbines creates noise effects that can annoy citizens.

6.2.2 Distance from the Grid

Another limitation is the proximity to the power grid. The solar PV plants are divided into two categories. 10-25 MW and 25 MW and above. A factor was assigned to assess the feasibility of the plant. For example, for plants over 25 MW, a distance of less than 10 km from the grid is considered optimal for plant placement. Anything over 50 km is exorbitant. Proximity to the power grid is a very important aspect to consider. Extending the power network can be very expensive and impact project profitability, so it makes sense to install the system in areas where infrastructure already exists. Additionally, bringing the new system closer to the consumer can reduce transmission losses.
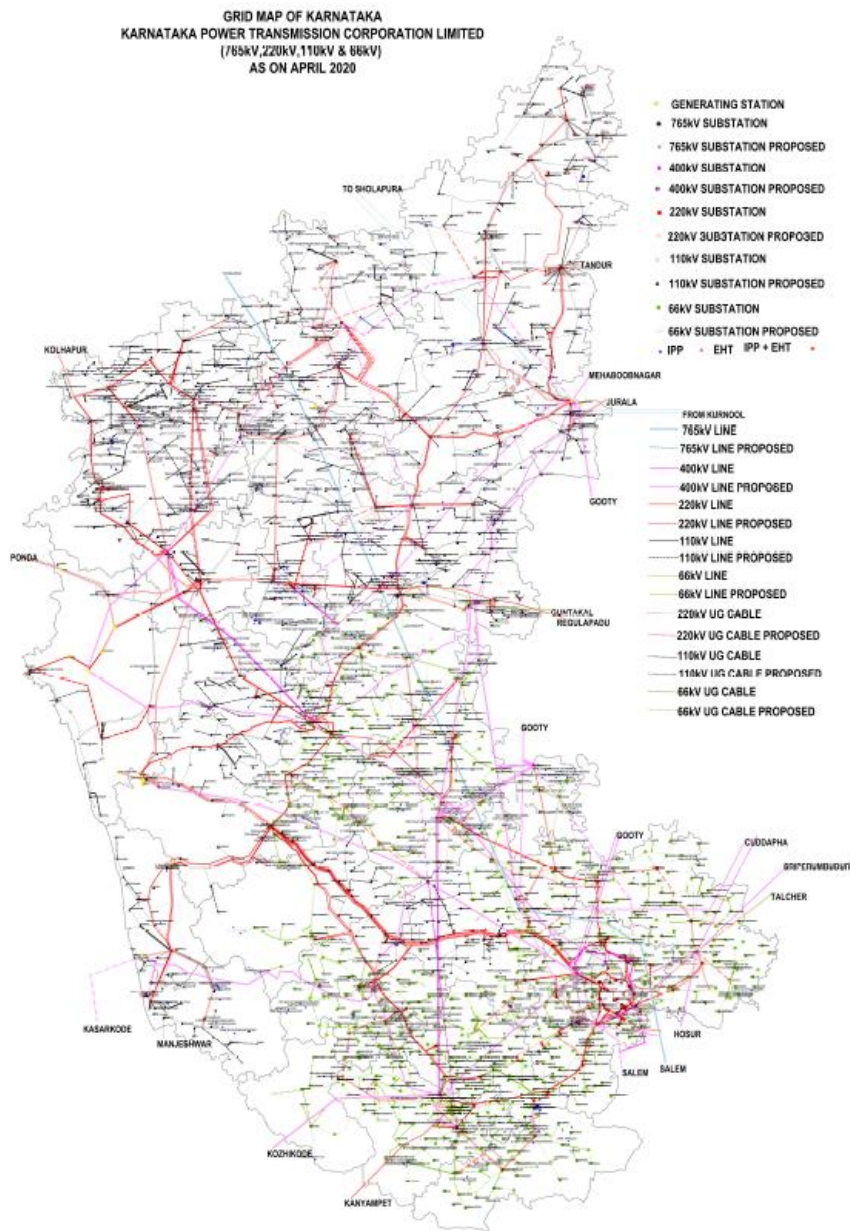
Figure 6-69 Transmission grid of Karnataka

6.2.3 Physical constraints

The main parameters that have to be analysed for selection of Installation sites for PV and Wind farms are, average global irradiance (>1500 kWh/m2), grid

proximity and for wind turbines average wind speed, roughness length and orography.

6.2.4 Site selection

To identify the possible installation sites of these plants, in a weighted analysis where all the constraints was carried out. A coefficient was associated with each constraint, based on its convenience, and with different specific weight. For example, the distance from the transmission grid has a higher percentage than the territorial constraints.

The sites selected are based on proximity to the transmission grid and therefore in proximity to a 220 kV or 132 kV lines. The selected area is near the city of Mysore. And the distance of the transmission grid from the selected area is approximately 8 kms. The roughness length(0.1m) and the orography(737m) is in the optimal range.

Figure 6-70 Installation sites
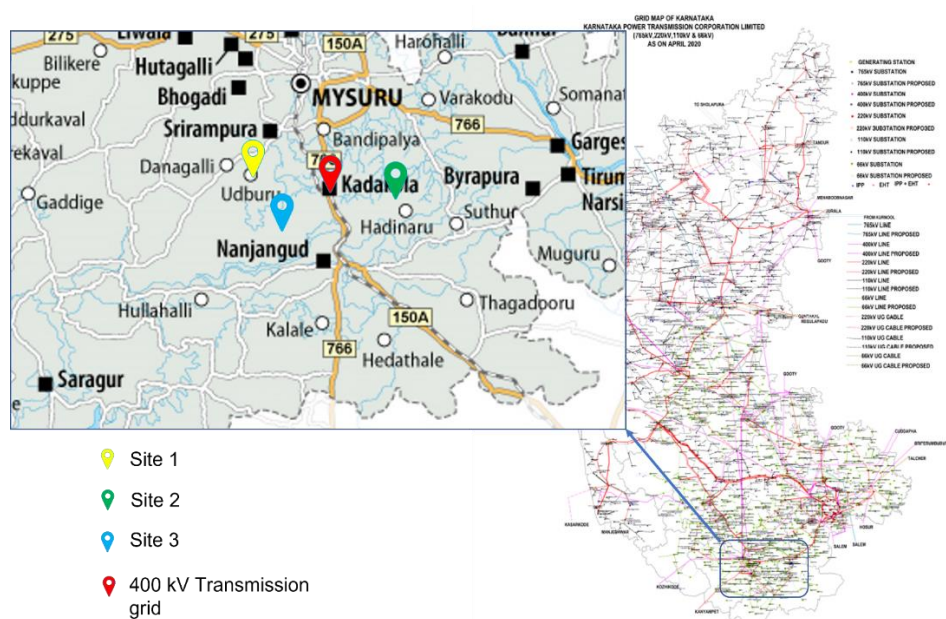
7 Energy policies

Indian government has taken many pioneering steps for Renewable energy improvements since 1987, began with the creation of the Indian Renewable Energy Authority (IREDA). Since output of wind power and solar power is in the form of electricity, their policy framework exhibits many similarities. Accelerated Depreciation (AD) policy, Viability Gap Funding (VGF), Power Purchase Agreement (PPA), Annual Power Purchase Cost (APPC), Feed-In Tariff (FIT) and Renewable Purchase Obligation (RPO) are the important components of Indian RE policy framework.

AD policy was announced in the 1990s for both wind and solar power projects allowing them to depreciate 100% of their debt in the first year of project commencement to reduce the interest amount and ultimately reduce the power generation cost. After 2014, the depreciation percentage was reduced to 80% indicating the growth of the RE-based power sectors [48]. Currently, the depreciation of 40% is permitted in the first year of the project implementations for wind and solar power projects. Hence, the same amount would be applicable to wind-solar hybrid power projects. The funding given to the project developers by the government to help in filling the gap between the available and required finance is termed as Viability Gap Funding(VGF). Currently, the VGF policy is not available for wind power generation . On the other hand, 30% of the project capital or INR 25 million/MW (whichever is lower) is given for solar power generation under VGF policy. Indian central government is increasing RPO every year to promote RE generation.[16]

FIT is the rate at which the generated electricity will be sold during the purchase agreement (PPA). India decides the FIT based on the reverse auction since 2017. FIT ranges between 0.052 $/kWh to 0.07 $/kWh.

Investment cost of PV	700 $/kW
Investment cost of WT	1100 $/kW
Investment cost of BESS	300$/kW
Operation and maintenance cost of PV	10 $/kW/year

Operation and maintenance cost of WT	0.0085 $/kW/year
Electricity selling price	0.052 $/kWh
Electricity buying price	0.1 $/kWh
Tax	1% of total investment

Table 7 Financial Data

8 Load Profile

The calculation of hourly load profile for the region of Karnataka was done with the help of the information obtained from other countries. The data, used for the simulation analysis is obtained from ENTSO-E and which refers to countries of Europe.

The temperature of the main cities in the region of Karnataka is almost similar to the cities in he European countries in the summer season, whereas the temperature of European countries during the Winter season is far more different from the temperature of Karnataka region in the winter season. In order to obtain the almost real hourly load profile for the region of Karnataka, the load profiles of the European countries for the summer months were used. And to adapt the load profile some correction factor, proportional to the annual electricity consumption of the region of Karnataka was calculated and referred.
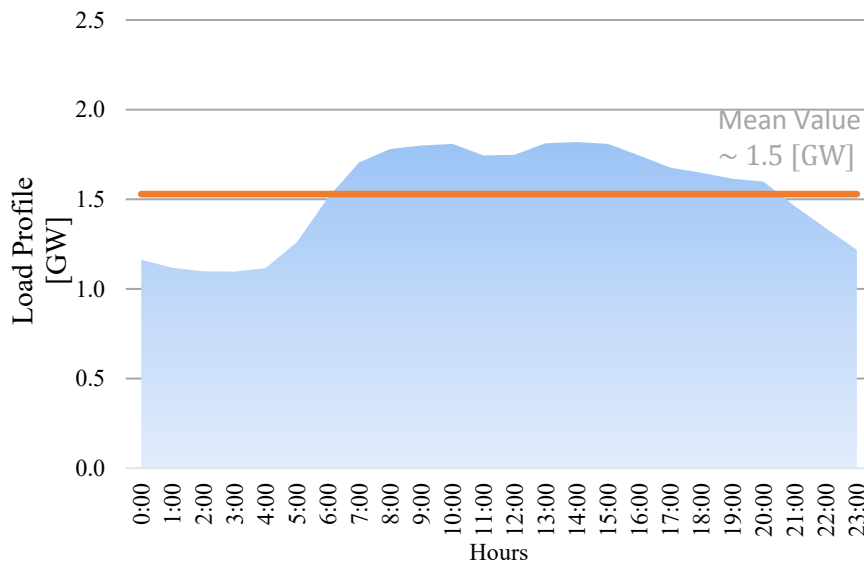
Figure 8-71 Representation of the hourly profile of a significant day

The above represents the hourly load profile of Italy for a significant day, obtained from the methodology described above. This above load profile is compared with the load profile for a significant day for the region of Karnataka.

After the comparison between the load data of Italy and that of for the region of Karnataka, shows some similarities. However, the load profile in some literature has peak leads at nights. With the help of correction factor the load profile is used for the calculations.

For the visualization purpose the weekly, monthly, and annual load profiles are calculated by the methods described above. From the below figures we can observe that the hourly load profile doesn't change during different seasons and as they are created by repeating the hourly profiles referring only to summer months.
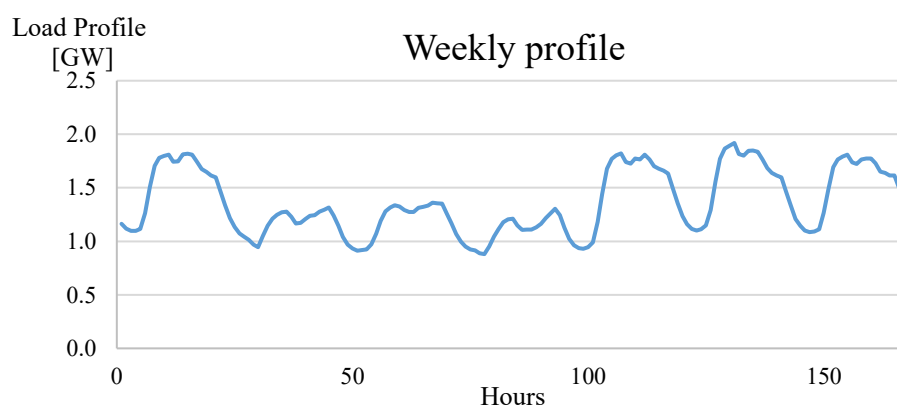
Figure 8-72 Calculated weekly load profile
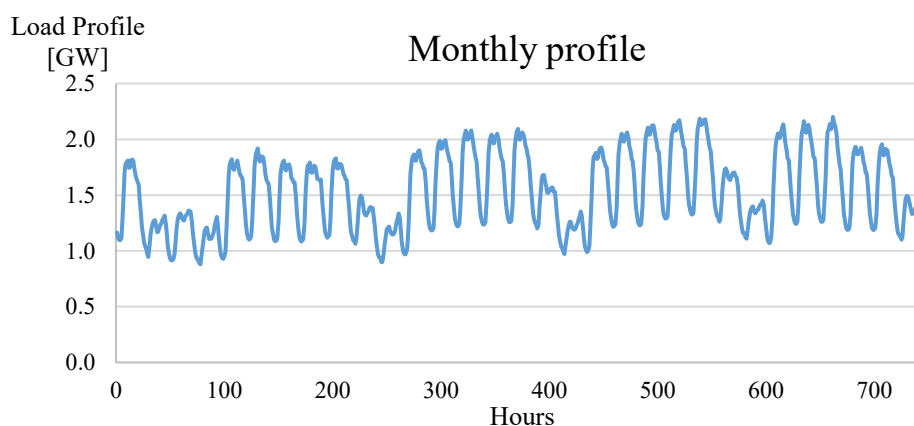
Figure 8-73 Calculated monthly load profile
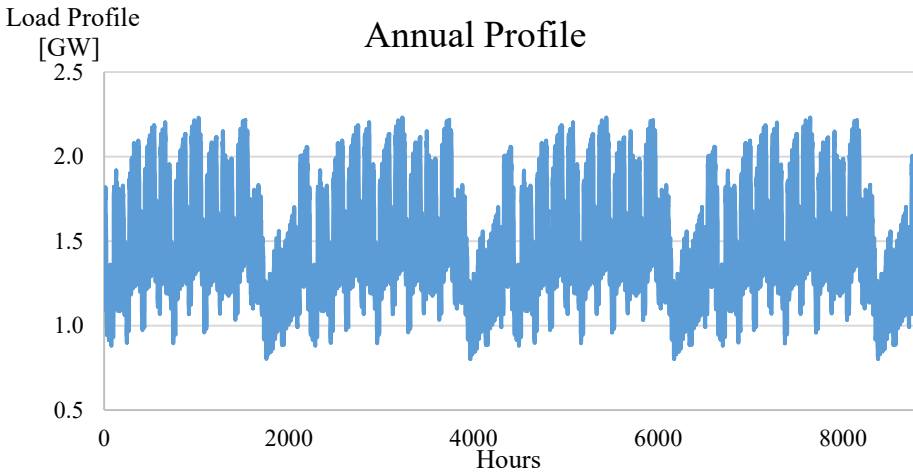
Figure 8-74 Calculated annual load profile

9 Case study: Optimal sizing of PV, WT and BESS in Karnataka, India

In this part of the thesis planning of optimal sizing of the RES plants thereby increasing its Self-sufficiency and IRR is performed and results are shown.

To perform this analysis of optimization it is important to exploit the information obtained in the above chapters. This analysis is performed, to the sites selected in the before sections and the financial data such as investment cost of PV, WT and BESS, operation and maintenance cost of PV, WT, BESS, Discount rate and Tax reduction are also indicated in previous sections and are used during the analysis.

9.1 Resource analysis

At the start the simulation is performed with 1MW capacity of PV and wind plant with 1MW BESS, the capacity of the plant is not so important at this step because, here we are going to analyse the productivity of the PV and wind plants at the selected location, and they are compared.

For the selected location the Irradiance data and wind speed data is analysed and compared with the data sets of other locations.

	2006	2007	2008	2009	2010	2011	2012	2013	2014	2015	2016
Dec	204.61	184.02	208.43	179.24	174.84	194.26	205.75	210.88	180.65	192.01	188.55
Nov	149.61	198.71	174.24	167.29	150.13	170.57	203.30	187.27	180.88	142.32	193.83
Oct	149.46	177.11	174.61	202.26	179.59	196.89	179.99	184.56	181.83	204.04	179.29
Sep	143.93	155.61	184.49	162.12	159.86	172.63	178.45	163.49	175.44	181.70	143.54
August	139.23	148.75	156.88	169.24	145.74	149.65	155.46	160.45	152.07	171.68	143.46
July	136.56	139.55	152.88	146.16	138.64	149.04	161.84	142.49	154.29	166.72	118.21
June	130.37	139.15	148.17	168.06	150.66	138.15	156.66	143.15	172.64	156.96	120.61
May	159.91	191.47	195.85	183.67	191.31	195.63	196.34	185.18	186.69	174.88	167.19
April	191.72	212.33	209.41	202.92	201.75	201.66	195.08	200.75	205.22	195.17	200.78
March	206.44	235.53	201.72	224.04	229.01	236.90	235.20	221.65	229.09	225.03	216.50
Feb	211.16	211.40	191.90	217.00	208.17	207.91	220.35	200.29	197.73	213.42	193.20
Jan	207.84	216.95	218.68	221.77	210.70	220.74	222.36	225.95	219.84	210.22	197.73

Total Yearly Global irradiance (kW/m2)

Figure 9-75 Irradiance data for each year

The above irradiance data is of the site 2, and from the above diagram we can observe that there is no much change in irradiance data over the different years. i.e. the irradiance value almost remains the same for different years.

	2006	2007	2008	2009	2010	2011	2012	2013	2014	2015	2016
Dec	2.92	3.10	2.67	2.64	2.59	2.51	2.78	2.68	2.36	2.61	2.18
Nov	2.08	2.21	2.48	2.43	2.15	2.67	2.24	2.20	2.18	2.18	1.84
Oct	2.26	1.95	1.83	2.44	2.82	2.09	2.53	2.78	1.99	2.36	1.94
Sep	3.16	3.59	3.08	3.05	3.73	4.56	3.81	3.83	3.53	3.11	3.35
August	4.29	3.84	3.42	3.59	4.85	5.30	4.59	4.22	4.20	3.83	4.00
July	5.56	4.41	4.00	5.36	5.43	5.84	4.96	5.77	5.44	4.51	4.07
June	3.82	3.93	4.26	3.88	5.09	6.18	5.14	5.49	4.76	4.55	3.73
May	3.05	2.32	2.32	2.21	3.34	3.13	3.22	3.28	2.83	2.45	2.12
April	1.83	1.74	1.81	2.02	2.27	2.19	2.30	2.15	2.17	1.70	1.42
March	1.86	2.20	2.20	1.96	2.68	2.63	2.33	2.16	2.46	2.22	1.56
Feb	2.60	2.27	2.27	2.37	2.40	2.31	2.60	2.37	2.14	2.50	1.94
Jan	2.66	2.77	2.47	2.69	2.58	2.72	2.14	2.35	2.85	2.28	1.96

Avg wind speed (m/s) Measured at height 10m

Figure 9-76 Wind data for each year

The above diagram represents the wind speed for the site 2 for different years, and from the above figure we can observe that the wind speed is high during the summer season and comparatively less in winter season.

From the results obtained during the first step, the productivity of PV plant is 1524 MWh/MW/year and productivity of WT farm is 1816 MWh/MW/year

9.2 Maximisation of self sufficiency

The main objective of this thesis to maximize, the self-sufficiency and the economic parameters such as NPV and IRR of the RES plant. In this paragraph we discuss about maximization of self-sufficiency performed by the RES tool.

Before optimizing the PV, WT and BESS sizes to increase the self-sufficiency of the plant, it is necessary to analyse some graphs of significant days, thereby we can understand the exchanges with the grid and the production profiles in comparison with loads.
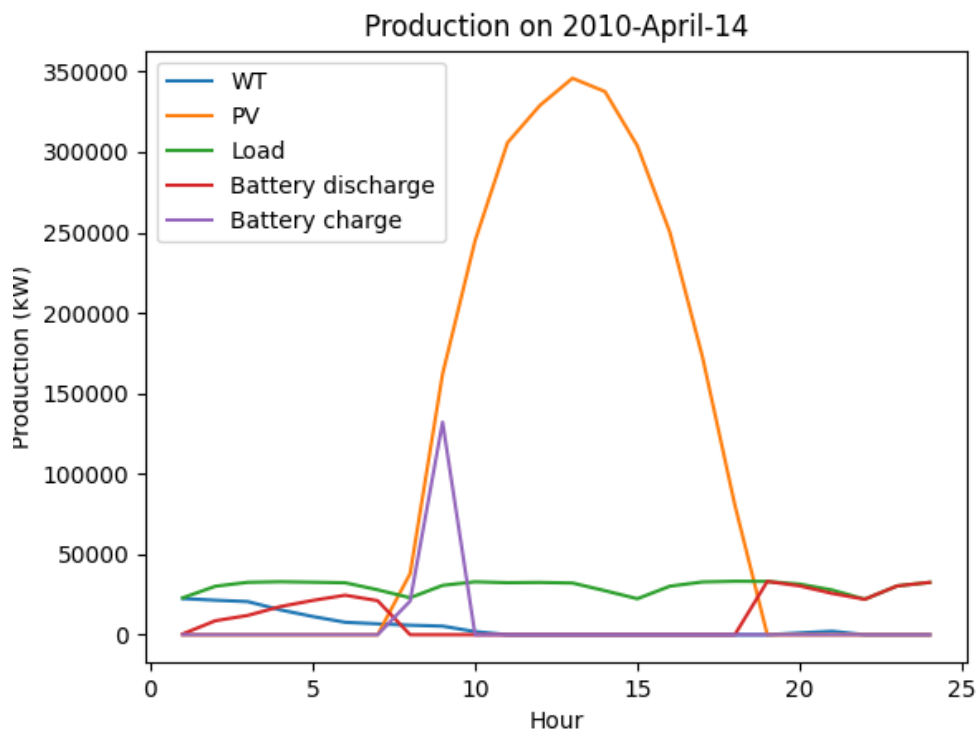

Figure 9-77 Daily profiles with use of the storage battery for a clear day

The above figure represents a clear sunny day, from the PV production graph we can observe that the production is well distributed throughout the day. In the morning until 8:00 a.m. we can observe that wind turbine production is lower than

the load and there is no production of PV plant, hence the battery is discharged to satisfy the load. Starting from 9:00a.m. PV plants starts its production, and its production is higher than that of load, therefore discharging of the battery is stopped and load is satisfied by the PV plant alone whereas there is very little or almost zero production of the wind turbine farms. After charging of BESS is fully completed, the excess energy is supplied to grid. In the above figure we can observe that after 19:00, there is no production of PV and WT plant, hence now the battery discharges again to satisfy the load. It is noted that on this day there is no absorption electricity from the grid, the RES plant is able to satisfy the load on its own.
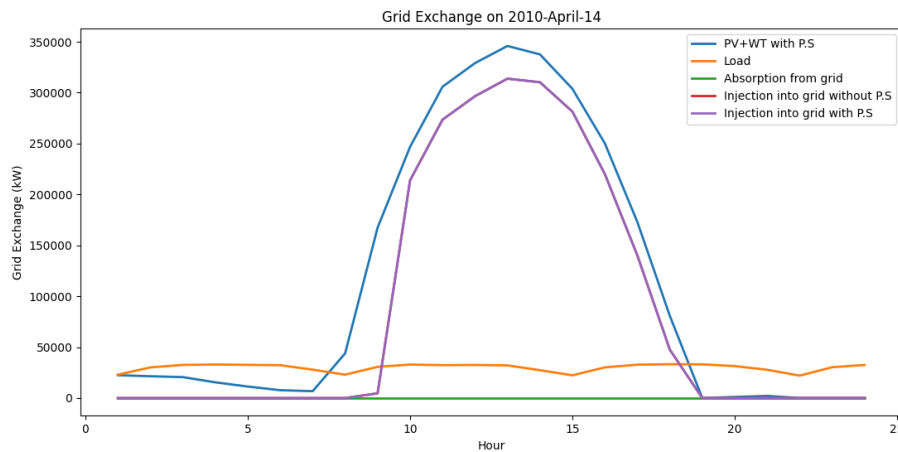

Figure 9-78 Daily profiles with exchanges with the grid for a clear day

From the above graph we can observe that the once PV plant completely satisfies the load and completely charges the BESS, the excess of electricity is supplied/injected to the grid.
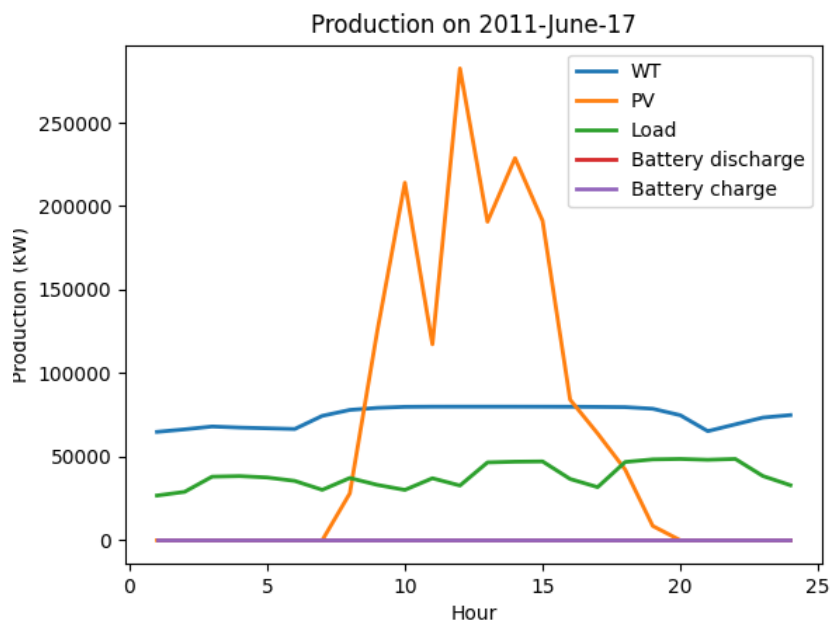
Figure 9-79 Daily profiles for a day with high availability of wind resource

For the selected co-ordinates, it was analysed that the month of June shows high wind resource. During this day all the load is satisfied by the WT plant and since the battery is fully charged, all energy produced by the PV plant is injected into the

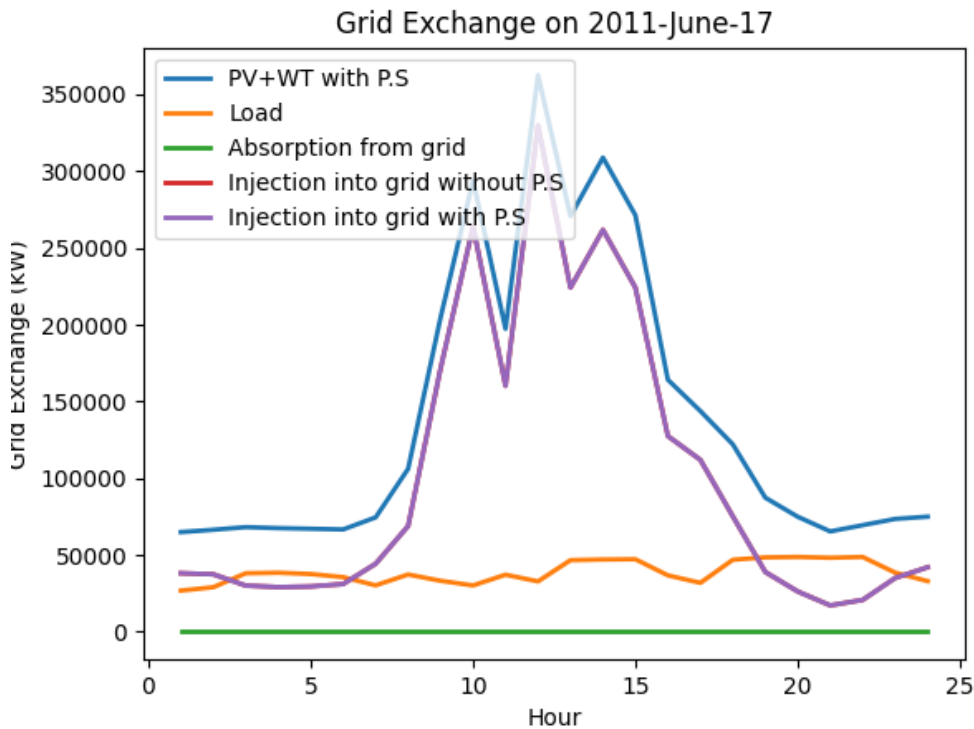grid,   and   it   is   show   in   below   figure.

Figure 9-80 Daily profiles with exchanges with the grid, for a day with high availability of the wind resource

To optimize the self-sufficiency of the plant, there is optimize function in the RES tool, through this function we can optimize the RES plant to maximize the self-sufficiency of the plant along with some economic constraints, here the IRR of the plant is constrained to a value. The application performs necessary steps to find the optimal capacity of RES plant to maximize the self-sufficiency of the plant, and not lowering the IRR of the plant below the value mentioned by the user.

To carry out this process, the user may provide max and min values of PV, WT and BESS capacities that are to be installed, and the user can also provide min value of the IRR. The tool performs necessary steps to find optimal solution there by not decreasing the value of IRR mentioned by the user.

The simulation was carried out for the site 1 and following constraints were imposed

	MIN	MAX
PV size (kW)	0	No limit
WT size (kW)	0	No limit
BESS size (kW)	0	No limit
IRR (%)	16%	NA
Max injection into grid(MW)	NA	100

Table 8 Constraints for Case 1

For case #1, max injection into grid = 100(GW), but this time the simulation was carried out only with PV generators, whereas the number of wind turbines is set to zero, and the results are tabulated.

For case #2, max injection into grid = 100(GW), but simulation was carried out only with wind turbines, whereas the size of the PV plant is set to zero. The results are tabulated.

For case #3 and #4, , max injection into grid = 100(GW), in this simulation both PV plant and wind turbines were considered, and simulation was done.

The simulation was carried out by the RES tool and results are tabulated below.

	Case 1	Case 2	Case 3	Case 4
	Site 1	Site 1	Site 1	Site 1
Limitation of the maximum injection [GW]	0.1	0.1	0.1	0.1
Total power of PV generators [GW]	0.2	0	0.1	0.1

Productivity of PV [GWh/GW/y]	1601	0	1601	1601
Total power of WT generators [GW]	0	0.2	0.1	0.1
Productivity of WT [GWh/GW/y]	0	2627	2627	2627
Capacity of storage [GWh]	0.3	0.3	0.75	0.3
Production from PV+WT [TWh/years]	0.316	0.45	0.41	0.41
Annual load [TWh/years]	0.314	0.314	0.314	0.314
Injection in the grid [TWh/years]	0.095	0.235	0.133	0.147
Absorption from the grid [TWh/years]	0.11	0.098	0.04	0.05
Grid exchange (abs.+inj.) [TWh/years]	0.20	0.333	0.17	0.2
Battery charge [GWh/years]	93.1	26.93	75.11	60.4
Battery discharge [GWh/years]	75.4	21.81	60.6	48.8
Self-consumption	64%	47%	65%	62%
Self-sufficiency	65%	72%	86%	82%
Absorption from the grid/load	35%	31%	14%	18%
Injection in the grid / load	30%	75%	42%	47%
Production from renewables/load	101%	145%	133%	133%
Initial investment [billion €]	-0.22	-0.31	-0.4	-0.27

NPV after 25 years [billion €]	0.105	0.038	0.17	0.36
IRR	9%	11.8%	16.36%	27.34

Table 9 Comparison of results of different cases

From the above table we can observe that self-sufficiency is high in case #3 and #4,but self-sufficiency of case #3 is slightly higher than that of case#4. When compared with economic parameters case#4 has better NPV and IRR values. Hence case#4 is considered as optimal result and it is used for planning of RES plant.
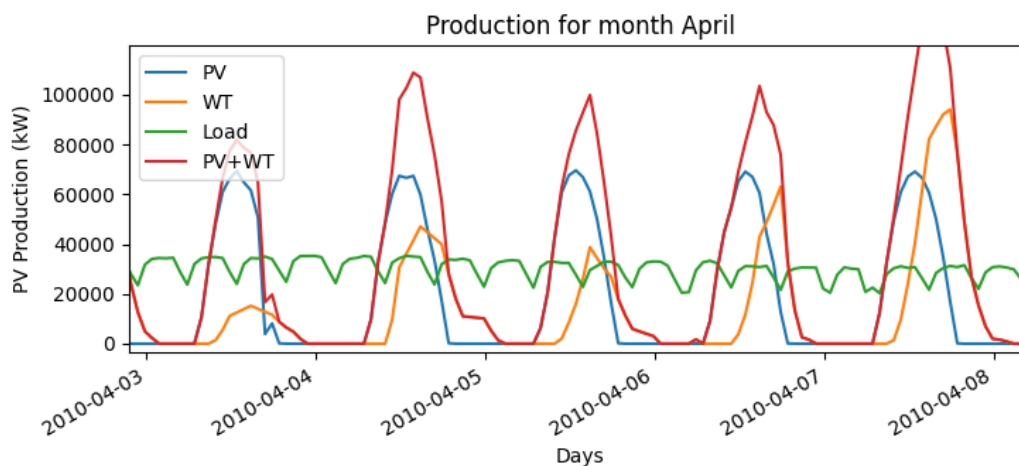

Figure 9-81 Maximization self-sufficiency, monthly profiles, Case #4

From the above figure we can observe that the combined RES production is higher than the load during the daytime, and PV plant produces most of the energy and this energy is used by the load and excess energy is used to charge the BESS, if the BESS is already completely charged, then this excess energy is injected into the grid and sold to the neighbouring regions. During the night-time energy produced by the wind farm is enough to satisfy the load. In some cases, we can observe that during the night-time, production of wind farm is less than that of load, hence BESS is allowed to discharge to satisfy the load. IF BESS is completely discharged then electricity is absorbed by the grid.
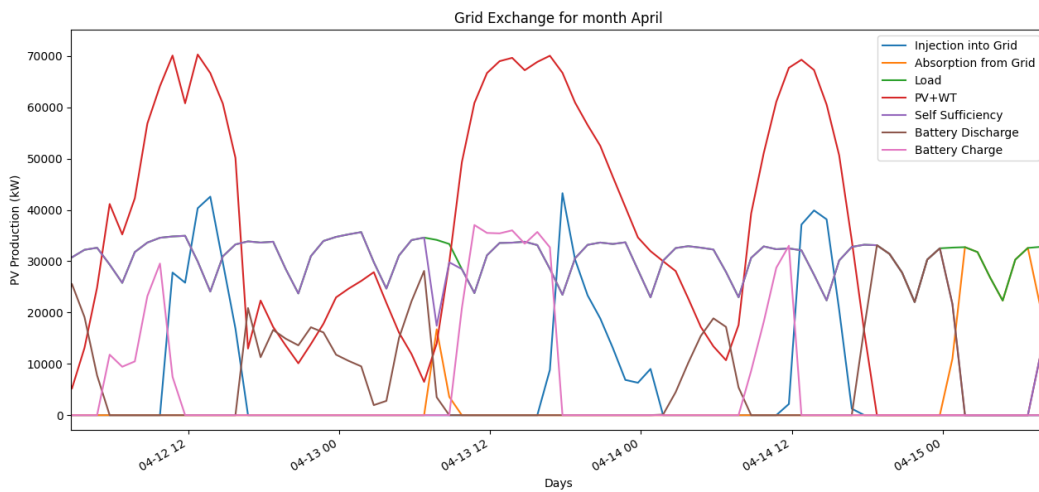
Figure 9-82 Maximization of self-sufficiency, monthly profiles with absorption and injection in the grid

From the above graph we can observe that energy produced by the PV and Wind plant is enough to satisfy the load . Hence no energy is absorbed from the grid, since we have implemented limitation on maximum injection of electricity into grid by 100 MW

Case#4 allows to maximize self-sufficiency, reaching 82%, but also allows to have an excellent economic return on investment. In fact, the NPV value calculated after 25 years is positive and the IRR is 27.3%. For the calculation of the NPV, the positive cash flows are those due to self-consumed energy and therefore not purchased from the external grid and from the sale of electricity to other country. In this case, the self-consumed energy was valued at 0.3 $/kWh and the selling price was instead equal to 0.028 $/kWh, both for PV systems and for wind systems. The negative cash flows are instead due to the initial investment cost and annual maintenance costs. *Figure 4.19* shows the calculation of the NPV, every 10 years battery of the plant is replaced, for this reason the curve is not always increasing and in the year 10 and 20 there are negative cash flows. The payback time (PBT) occurs after about 5 years, which is seen clearly in the below graph.
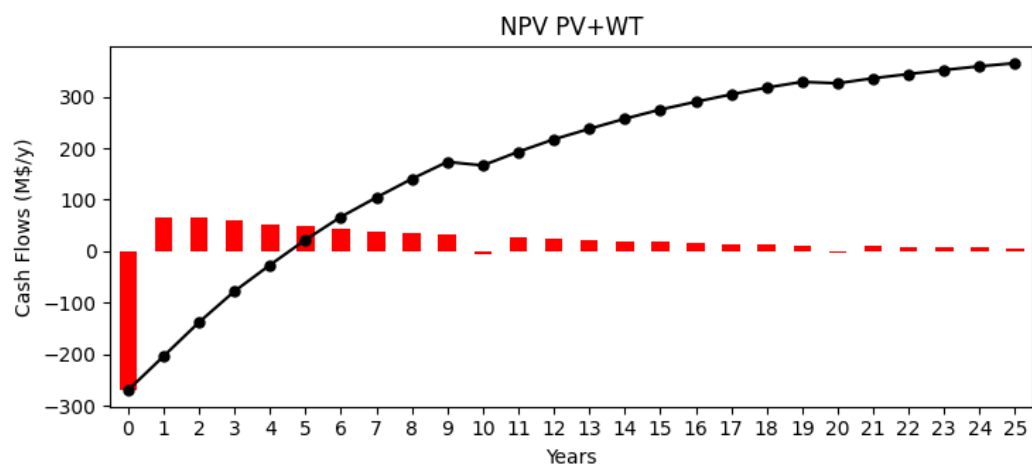
Figure 9-83 Maximization of self-sufficiency, NPV trend for Case #4

10   Conclusion

The optimal planning of RES plant, i.e., optimal planning of PV plant, Wind farm and BESS is performed by keeping in consideration of physical and economic constraints. And this planning is done for the region of Karnataka in India.

First, selection of RES installation sites was carried out by considering territorial constraints, and distance of grid from the RES plant. Then resource analysis was performed by analysing the data of irradiance, wind speed.

The ultimate goal of this thesis work is to plan a RES system for the region of Karnataka, and to make it independent as much as possible from the use of fossil fuels. And the economic return of the plant is also considered, so that the system can be planned in such a way that, it is profitable. Hence for this analysis, site 1 is selected, and different simulations are performed with different constraints. The RES tool produced optimal results for the selected site, by improving self-sufficiency of the RES plant to be 82% and this is achieved by installing PV plant size of 100MW and 50 number of WTG and with BESS of size 300 MW with IRR is limited to 27.3% and NPV of the plant is 365 million $.

The most favourable plant is the one that allows to produce everything that is self-consumed by the load, thereby avoiding the use of fossil fuels and also the purchase of electricity from neighbouring countries. The solution found by maximizing the IRR is an excellent compromise between self-sufficiency and NPV value obtained. At last, in this case, the solution obtained by maximizing the value of self-sufficiency was preferred.

11   References

[1] F. Spertino, Lezioni di "Sistemi per la produzione dell'energia elettrica"
- Politecnico di Torino, A.A. 2011/2012;

[2] F. Spertino e R. Carelli, "Impianti fotovoltaici di piccola taglia", CLUT,
2008;

[3] F. Spertino e A. Abete, "Generatori e Impianti Fotovoltaici", Dip.
Ingegneria Elettrica, Politecnico di Torino, CELID, 2001;

[4] F. Spertino, "Conversione Fotovoltaica dell'Energia", Dip. Ingegneria
Elettrica, Politecnico di Torino, Dispensa 2010;

[5]F. Spertino e A. Abete, "Appunti vari dalle lezioni", Dip. Ingegneria
Elettrica, Politecnico di Torino, A.A. 2009/2010;

[6] F. Spertino, "Guida all'integrazione architettonica delle installazioni
solari negli edifici", 2011;

[7] M. Nobile, "*Regolazione di tensione nei sistemi di bassa tensione
tramite On Load Tap Changer e altri dispositivi di regolazione*" 2021,
Politecnico di Torino.

[8] A. DeMatteis, "L*'integrazione dei sistemi fotovoltaici negli
edificipubblici: caso studio con flussi energetici e convenienza
economica*" July 2016, Politecnico di Torino.

[9] F.Spertino, «course slide: *Photoviltaic systems*»2020, Politecnico di
Torino.

[10] G. Bracco, «course slide: *Wind and Ocean Energy Plants*» 2020,
Politecnico di Torino.

[11] F.Spertino, «course slide: : *Wind and Ocean Energy Plants* »2020,
Politecnico di Torino.

[12] M. Santarelli, «course slide: NOTES ON CLOSED BATTERIES,
Polygeneration and advanced energy system» 2020, Politecnico di
Torino.

[13] E. Chiavazzo, «course slide: *Energy storage*» 2020, Politecnico di Torino.

[14] A. Ciocia*, "Optimal Power Sharing between Photovoltaic Generators, Wind Turbines, Storage and Grid to Feed Tertiary Sector Users",* Doctoral Dissertation, Doctoral Program in Electrical and Communications Engineering (29th Cycle), 2017.

[15] Alok Das, Hardik K. Jani, Garlapati Nagababu, Surendra Singh Kachhwaha, A comprehensive review of wind–solar hybrid energy policies in India: Barriers and Recommendations, Renewable Energy Focus, Volume 35, 2020, Pages 108-121.

[16] P. Balachandra, Darshini Ravindranath, N.H. Ravindranath, Energy efficiency in India: Assessing the policy regimes and their impacts, Energy Policy, Volume 38, Issue 11, 2010, Pages 6428-6438.